uOttawa

L'Université canadienne
Canada's university

FACULTÉ DES ÉTUDES SUPÉRIEURES ET POSTOCTORALES

uOttawa

L'Université canadienne
Canada's university

FACULTY OF GRADUATE AND POSDOCTORAL STUDIES

Hsin-Hua Wei

AUTEUR DE LA THÈSE / AUTHOR OF THESIS

M.Sc. (Mathematics)

GRADE / DEGREE

Department of Mathematics and Statistics

FACULTÉ, ÉCOLE, DÉPARTEMENT / FACULTY, SCHOOL, DEPARTMENT

Population Dynamics of Central Place Foragers

TITRE DE LA THÈSE / TITLE OF THESIS

Frithjof Lutscher

DIRECTEUR (DIRECTRICE) DE LA THÈSE / THESIS SUPERVISOR

CO-DIRECTEUR (CO-DIRECTRICE) DE LA THÈSE / THESIS CO-SUPERVISOR

Victor Leblanc

Tom Sherratt

Gary W. Slater

Le Doyen de la Faculté des études supérieures et postdoctorales / Dean of the Faculty of Graduate and Postdoctoral Studies

Population Dynamics of Central Place Foragers

Hsin-Hua Wei

Thesis Submitted to the Faculty of Graduate and Postdoctoral Studies
In partial fulfilment of the requirements for the degree of Master of Science in Mathematics [1]

Department of Mathematics and Statistics
Faculty of Science
University of Ottawa

[1]The M.Sc. program is a joint program with Carleton University, administered by the Ottawa-Carleton Institute of Mathematics and Statistics

Your file Votre référence
ISBN: 978-0-494-69100-7
Our file Notre référence
ISBN: 978-0-494-69100-7

Abstract

In this thesis we use analysis and simulation to study the qualititative behavior of several mathematical models for consumer-resource interaction. While such models have been studied for several decades now, our approach to include a random-walk model for the foraging behavior of the consumer is novel. With this approach we are able to link individual movement rules to population-level patterns.

For every species, acquisition and assimilation of food is an important process that enables survival, growth, and reproduction. Different species have developed different strategies for this process. Individuals who depart from one location on foraging trips and return to the same location are called central place foragers. Examples include cave crickets, beavers, and colonial seabirds. Resources around central place foragers' habitats are the major source of food. In this thesis, we consider discrete-time consumer-resource models and examine the following questions: (1) Under what conditions can consumers and resources stabily coexist? (2) How does the distribution of consumers affect resource abundance spatially? (3) How does the abundance and distribution of resource affect the foraging behavior of consumers?

First, we study a non-spatial model by considering that consumers disperse evenly over the resource patch. We apply several different functions for resource growth (compensatory and overcompensatory), and we consider various foraging behaviors (random versus clumped). We analyze the stability behavior of steady states in each of these models and we summarize our results in bifurcation diagrams. Next,

we study the spatial model by assuming that consumers tend to concentrate closer to the central place. We apply the Laplace distribution to describe consumers' dispersal. We focus on the compensatory dynamics for resource growth and consider both random search and clumped search for resources. In this section, we use a combination of analytical and numerical techniques to study the qualitative behavior of the system. Finally, we apply a random-walk framework to derive the distribution of consumers based on individual movement rules and the abundance of resources. That is, we have different consumer distributions depending on local resource abundance at different times. The analysis of this complex model is exclusively based on numerical simulation. For all consumer-resource models, we present one-parameter bifurcation diagrams for each parameter in the model to illustrate the qualitative behavior. We investigate the effects of parameters on the stability of steady states and limit cycles.

For models with fixed consumer distributions, we find that the clumped search for resources stabilizes the system. The resource and consumer populations can reach stable steady states if consumers aggregate intensively at the place with more abundant resources. We find that a resource-dependent distribution of consumers also stabilize the system as consumers settle at a more resource-rich location to forage. All parameters in our models have impacts on the population dynamics of resource and consumer. For the compensatory resource growth, we find that consumers can invade the system and both populations can reach a stable steady state for a higher value of resource growth rate or a lower value of consumer conversion efficiency. Other parameters can have different impacts on stability depending on different model structures.

Contents

List of Figures

List of Symbols

r : net reproductive rate

s : consumer survival rate

$\tilde{b}$: conversion efficiency from resource biomass to consumer biomass

L : patch size

a_F : consumer's searching efficiency

K : resource carrying capacity

a_R : energy reduction coefficient

α_L : scale parameter for the Laplace distribution

a : settling rate

D : diffusion coefficient

α : maximum settling rate

β : half-saturation constant

γ : constant related to the maximum slope of $a(F)$

Chapter 1

Introduction

Central place foragers are animals who depart from one location to the foraging patch and return to the same location [26]. Examples include cave crickets [9], beavers [29], and colonial waterbirds [30]. The question of how an individual central place forager should forage in order to optimize its net energy gain has long been studied. For example, the Marginal Value Theorem [4] [27] is conerned with the question of how long a forager should stay in patch before moving on to other patches. Charnov [4] stated that "the predator should leave the patch it is presently in when the marginal capture rate in the patch drops to the average capture rate for the habitat". In other words, a forager should stay in a patch as long as its marginal rate of food intake is at least equal to what it could capture in other patches, given that it has to pay a cost to travel to other patches (Chapter 10 in [6]). The formulation of the Marginal Value Theorem obviously assumes that the consumer has the knowledge of average food availability in different patches. This assumption is not always satisfied, many consumers need to make decisions based on local knowledge only. While much work was done on optimality of foraging strategies, very little attention was paid to how certain foraging strategies on the individual level affect the dynamics on the population level.

In this thesis we are most interested in the dynamics of populations depending on foraging strategies. In particular, we will derive and analyze an individual random walk model, where consumers decide to forage based on local information only, and we will investigate the population-level effects of individual movement rules. We start by giving an overview of various consumer-resource models and the mathematical techniques needed to study thesis.

Population dynamics has been studied intensively in the mathematical literature. The principal aim in studying models for species dynamics and interactions is to explain the distribution and abundance of biological populations (Chapter 1 in [13]). For a single population, Verhulst [32] (as quoted in Chapter 1 in [21], and Chapter 4 in [34]) proposed that a self-limiting process should operate when the population becomes too large, and he derived the logistic growth function. Later, Lotka [17] [18] and Volterra [33] developed a predator-prey model for two interacting populations. All these models are based on ordinary differential equations, i.e. they consider time to be continuous. Many biological populations from insects to mammals show strong seasonality, where for example all births occur over a short period of time only once a year. For such situations, a discrete-time modeling framework may be better suited. Nicholson and Bailey [23] produced such a model for host-parasitoids interaction. Their model has since been a starting and reference point for many discrete-time consumer-resource models. The work presented here also belongs to this category.

In this chapter, we do the following. We introduce the general form of our consumer-resource model which contains three mechanisms: (1) resource growth, (2) resource consumption, and (3) consumer survival. Then we give an overview of some typical functional forms that can be particularly applied to the model describing central place foragers and the resource.

We consider that central place foragers (consumers) have breeding seasons (for example, penguins [5] or white storks [14]), so the difference equations model is appropriate. We assume that within one generation, the resource grows first, then the

consumer comes to forage. The general form of consumer-resource model is (Chapter 4 is [22]), (Chapter 3 in [7])

$$F_{t+1} = G(F_t)[1 - p(F_t, C_t)] \tag{1.0.1}$$

$$C_{t+1} = \hat{b}G(F_t)p(F_t, C_t), \tag{1.0.2}$$

where F_t and C_t are the densities of resource and consumer at generation t, respectively. The function G is the resource growth function and the probabilty function p represents the probability of resource being consumed successfully. The number of consumer's offsprings depends upon the amount of resource consumed in the previous generation and $\hat{b}$, which can be interpreted as a conversion coeffcient relating consumed biomass to new adult consumers.

In the following, we describe several possible choices for the functions G and p. We consider the dynamics of the resource alone in section 1.1. Then we consider the ways in which a consumer forages in the system in section 1.2. In section 1.3, we present the most important methods to analyze the stability of the system.

1.1 Resource Growth

The resource grows according to some function G such that

$$F_{t+1} = G(F_t). \tag{1.1.1}$$

There are two fundamentally different types of growth functions: compensation or overcompensation. The compensatory function is a monotonically increasing function with a decreasing slope (Figure 1.1 and Figure 1.2). An increase in population reduces the per capita reproduction but not the total recruitment. In contrast, the overcompensatory function increases until it reaches to its maximum then decreases monotonically to zero (Figure 1.3 and Figure 1.4). An increase in population beyond the maximum reduces the total recruitment of the population.

Definition 1.1.1 *(Chapter 2 in [1]) For the first-order difference equation,*

$$x_{t+1} = f(x_t),$$

an equilibrium point (steady state) is a constant solution x^* to the difference equation, i.e. a solution x^* satisfying

$$x^* = f(x^*).$$

Definition 1.1.2 *(Chapter 2 in [1]) An equilibrium point x^* is locally stable if, for any $\epsilon > 0$, there exists a $\delta > 0$ such that if $|x_0 - x^*| < \delta$, then*

$$|x_t - x^*| < \epsilon,$$

for all $t \geq 0$. The equilibrium point x^* is locally attracting if there exists $\gamma > 0$ such that for all $|x_0 - x^*| < \gamma$,

$$\lim_{t \to \infty} x_t = x^*.$$

The equilibrium point x^* is locally asymptotically stable if it is locally stable and locally attracting.

Theorem 1.1.3 *(Chapter 2 in [1]) Assume f' is continuous on an open interval I containing x^* and x^* is an equilibrium point of f. Then x^* is a locally asymptotically stable equilibrium of $x_{t+1} = f(x_t)$ if*

$$|f'(x^*)| < 1$$

and x^* is unstable if

$$|f'(x^*)| > 1.$$

In this work, we are only concerned with local asymptotic stability, which we will also call "stable" for the sake of brevity. In the following growth functions, parameter K is the carrying capacity and r is the net reproductive rate at low density.

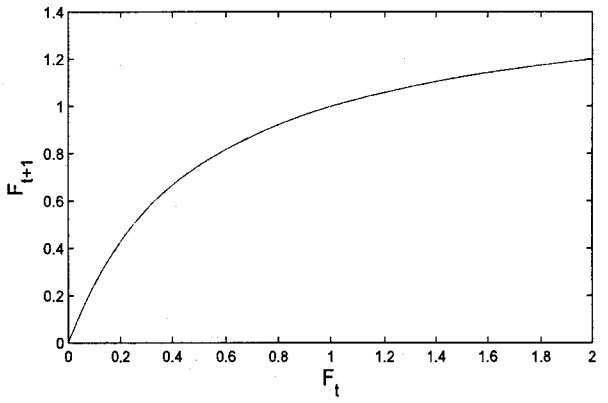

Figure 1.1: Beverton-Holt growth function at $K = 1$, $r = 3$.

1.1.1 Beverton-Holt

The Beverton-Holt equation was first introduced in the context of fisheries in 1957. The equation reads

$$F_{t+1} = G(F_t) = \frac{rKF_t}{K + (r-1)F_t}. \tag{1.1.2}$$

It is compensatory and continuously differentiable. It is a monotonically increasing hyperbolic function (Figure 1.1). The equilibria of the Beverton-Holt equation are $F^* = 0$ and $F^* = K$, which can be obtained by setting $F_{t+1} = F_t = F^*$.

According to Theorem 1.3, we can determine the stability of the equilibrium by investigating

$$G'(F^*) = \frac{rK^2}{[K + (r-1)F^*]^2}. \tag{1.1.3}$$

At $F^* = 0$, $G'(F^*) = r$ and it is unstable for $r > 1$ where we assume r is positive for biological reality. At $F^* = K$, $G'(F^*) = \frac{1}{r}$. Therefore, for $r > 1$, this non-trivial equilibrium is stable: a small pertubation from the carrying capacity K still leads the population back to K.

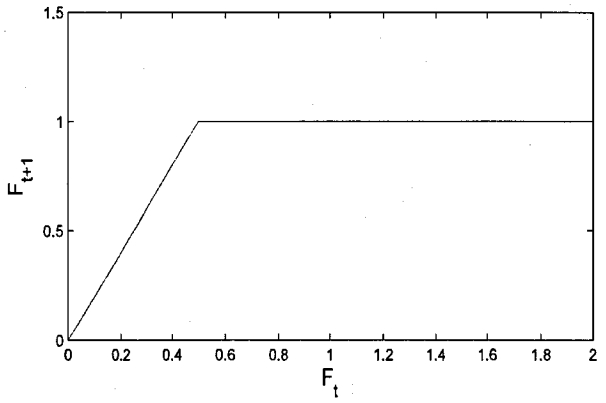

Figure 1.2: Holling Type 1 growth function at $K = 1$, $r = 2$

1.1.2 Holling Type 1

Holling (1959) considered a functional response of predator to prey [12] [13]. The number of prey eaten per predator increases as prey density increases, up to some limiting value representing the maximun possible prey consumption within the prescribed time. The Holling type 1 function increases linearly to a plateau as shown in Figure 1.2.

$$F_{t+1} = G(F) = \begin{cases} rF, & rF < K, \\ K, & rF \geq K. \end{cases} \tag{1.1.4}$$

It is also compensatory and is similar to the Beverton-Holt function. We will use this function in Chapter 3 to obtain explicit expressions for steady states of the consumer-resource model.

Similar to the Beverton-Holt function, Holling type 1 function also has two equilibria: $F^* = 0$ and $F^* = K$. By examining

$$G'(F^*) = \begin{cases} r, & rF^* < K, \\ 0, & rF^* \geq K, \end{cases} \tag{1.1.5}$$

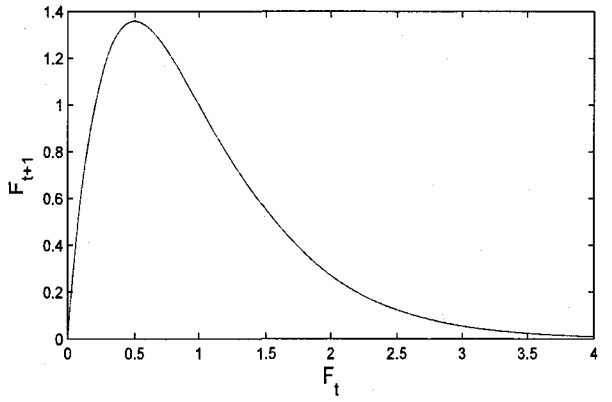

Figure 1.3: Ricker growth function at $K = 1$, $r = 2$

we know that the non-trivial equilibrium is unstable and the trivial equilibrium is stable for $r > 1$.

1.1.3 Ricker

W. E. Ricker developed the following function in his studies of stock and recruitment in fisheries [28] (Chapter 4 in [16]).

$$F_{t+1} = G(F_t) = F_t e^{(r-1)(1-\frac{F_t}{K})} \tag{1.1.6}$$

The Ricker function is overcompensatory as shown in Figure 1.3. It has two equilibria $F^* = 0$ and $F^* = K$.

Since the Ricker function is continuously differentiable, and

$$G'(F^*) = (1 - \frac{r-1}{K}F^*)e^{(r-1)(1-\frac{F^*}{K})}, \tag{1.1.7}$$

the trivial equilibrium is unstable for $r > 1$. At the non-trivial equilibrium, $G'(K) = 2 - r$. The equilibrium at the carrying capacity K is thus stable for $1 < r < 3$.

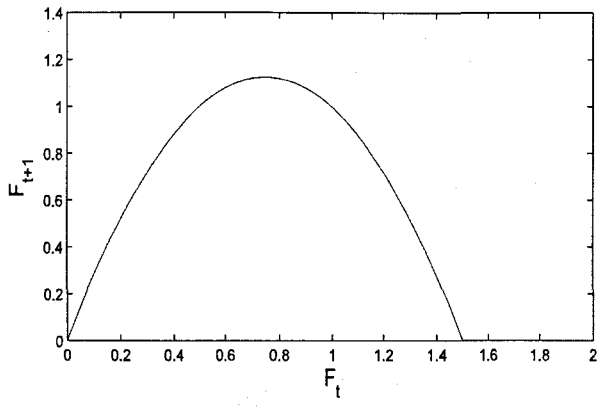

Figure 1.4: Logistic growth function at $K = 1$, $r = 2$

1.1.4 Logistic

The logistic equation, first published by Pierre Verhulst, is commonly applied to describe population growth (Chapter 4 in [16]). It is given by

$$F_{t+1} = G(F) = rF_t - \frac{r-1}{K}F_t^2. \tag{1.1.8}$$

The logistic function is concave-down, parabolic and overcompensatory as shown in Figure 1.4. It also has two equilibria: $F^* = 0$ and $F^* = K$.

Similarly, the Logistic function is continuously differentiable and the stability of these two equilibria can be determined by investigating

$$G'(F^*) = r - 2\frac{r-1}{K}F^* \tag{1.1.9}$$

Since $G'(0) = r$, the trivial equilibrium is unstable for $r > 1$. For the non-trivial equilibrium, $G'(K) = 2 - r$. Thus,the carrying capacity K is stable for $1 < r < 3$. According to May's review article [19], for $1 < r < 2$, pertubations from the non-trivial equilibrium tend monotonically toward the carrying capacity. For $2 < r < 3$, small pertubation still returns to the non-trivial equilibrium but in an oscillatory manner since $G'(r) < 0$ for $2 < r < 3$.

Both compensatory and overcompensatory equations above have the same equilibria: a trivial equilibrium $F^* = 0$ and a non-trivial equilibrium $F^* = K$. To avoid species from extinction, the net reproductive rate r must be grater than 1; i.e. each individual has to leave more than 1 offspring before dying. Hence, by assuming $r > 1$, the trivial equilibrium for the above equations are all unstable. For compensatory equations, the non-trivial equilibrium is stable for all $r > 1$. However, for the overcompensatory equations, this non-trivial equilibrium is stable only for $1 < r < 3$.

1.2 Probability of Consumption

We assume that the probability of resource consumed is propotional to the density of consumers. In addition, we consider that the probability also depends upon some parameter a_F, that can be interpreted as the consumer's searching efficiency.

1.2.1 Negative Exponential

Consumers may search for resource at random, or they may aggregate to a more resource-rich place. The Poisson distribution is a discrete probability distribution that expresses the probability of a number of random events occurring in a fixed period of time. The probability of n events is

$$q(n) = \frac{e^{-\mu}\mu^n}{n!} \tag{1.2.1}$$

where μ is the average number of events in the given time interval. In our case, we consider $q(n)$ as the probability that a resource is being found n times. The parameter is propotional to the consumer density, i.e. $\mu = a_F C$, where C is the consumer density. Then the probability that the resource escapes from consumption is

$$q(0) = e^{-a_F C}. \tag{1.2.2}$$

Equation (1.2.2) is commonly used in the Nicholson-Bailey model, which we discuss in section 1.4. We apply a negative exponential

$$p(C) = 1 - q(0) = 1 - e^{-a_F C} \tag{1.2.3}$$

as the probability of resource being consumed in our model.

1.2.2 Negative Binomial

May adopted the negative binomial function to describe the distribution of parasitoid encounters with hosts by [20] [12]

$$q(0) = \left(1 + \frac{a_F C}{m}\right)^{-m}. \tag{1.2.4}$$

where the parameter m captures the degree of parasitoid aggregation. Parasitoid aggregation is weaker as m increases. This probability becomes the negative exponential function derived from the Poisson distribution if $m \to \infty$. It follows the limit definition of e: $\lim_{x\to 0}(1+x)^{1/x} = e$. If the parasitoids disperse uniformly in the domain, aggragation is the weakest and the model with the negative binomial probability is equivalent to the one with the negative exponential probability.

At the other extreme, for $m = 1$ we have strong aggregation, so that

$$p(C) = 1 - \frac{1}{1 + a_F C}. \tag{1.2.5}$$

This form is also analytically tractable, see Chapters 3 and 4.

1.3 Stability Analysis

In nature, various types of population dynamics are observed. Some species persist and some go extinct. Some populations reach an equilibrium after several generations and some have a cyclic or chaotic behavior. Interestingly, these phenomena can be explored in mathematical models.

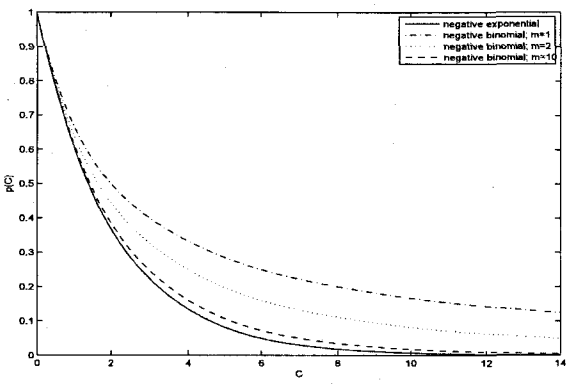

Figure 1.5: Negative exponential and negative binomial functions at $a_F = 0.5$, $m = 1, 2, 10$. As the aggregation degree of negative binomial function increases, the curve of negative binomial function is closer to the curve of negative exponential function.

Consider an autonomous consumer-resource system of the form

$$F_{t+1} = g(F_t, C_t), \tag{1.3.1}$$

$$C_{t+1} = h(F_t, C_t). \tag{1.3.2}$$

Over long periods, the solutions F_t and C_t might converge to equilibria, oscillate within a bounded range (limit cycles), or behave chaotically. Similar to the single-species model, equilibria for consumer-resource model are obtained by solving

$$F^* = g(F^*, C^*), \tag{1.3.3}$$

$$C^* = h(F^*, C^*). \tag{1.3.4}$$

To analyze the stability of each equilibrium, we linearize the functions g and h about the equilibrium and write the linearized functions into a matrix form

$$J = \begin{bmatrix} \frac{\partial g}{\partial F} & \frac{\partial g}{\partial C} \\ \frac{\partial h}{\partial F} & \frac{\partial h}{\partial C} \end{bmatrix}. \tag{1.3.5}$$

The Jacobian matrix J captures the stregth of the interaction in a community at the equilibrium (Chapter 8 in [16]). The corresponding characteristic polynomial is

$$P(\lambda) = \lambda^2 - \mathrm{tr}(J)\lambda + \det(J). \tag{1.3.6}$$

The trace and determinant of J determine the eigenvalues λ.

Theorem 1.3.1 *(Chapter 2 in [1]) Assume the functions $g(F,C)$ and $h(F,C)$ have continuous first-order partial derivatives in F and C on some open set in $\mathbb{R}^2$ that contains the point (F^*, C^*). Then the equilibrium (F^*, C^*) of the nonlinear system*

$$\begin{aligned} F_{t+1} &= g(F_t, C_t), \\ C_{t+1} &= h(F_t, C_t), \end{aligned}$$

is locally asymptotically stable if the eigenvalues of the Jacobian matrix J evaluated at the equilibrium satisfy

$$|\lambda_i| < 1$$

and (F^*, C^*) is unstable if $|\lambda_i| > 1$ for some i.

As parameters of the model change, so do the eigenvalues. If the stability of a steady state changes with a change in parameters, we call this a (local) bifurcation. Hence, bifurcations can happen only if $|\lambda| = 1$. The following considerations about bifurcations are important for the reminder of this work.

1.3.1 Bifurcation

A simple nonlinear difference equation can possess a remarkable spectrum of dynamics [19]. A dynamical system may have stable equilibria, stable cycles, or chaotic phenomena. A bifurcation could be a period doubling, quadrupling, etc., that accompanies the appearance of chaos. It represents the sudden qualitative change in the model's behaviour when varying the parameters (Chapter 3 in [11]), (Chapter 3 in

[31]). The following three bifurcations appear repeatedly in our work: transcritical, flip, and Neimark-Sacker bifurcation.

Definition 1.3.2 *A bifurcation is said to be the transcritical bifurcation if the stability of one stable equilibrium and one unstable equilibrium exchange when they collide. For a transcritical bifurcation, the number of steady states is not changed and we necessarily have* $\lambda = 1$.

Example 1.3.3 Consider

$$x_{t+1} = f(x_t, \mu) = x_t + \mu x_t - x_t^2. \tag{1.3.7}$$

We can verify that $(x^*, \mu) = (0, 0)$ is an equilibrium with eigenvalue 1, i.e.,

$$\begin{aligned} f(0,0) &= 0, \\ \frac{\partial f}{\partial x_t}(0,0) &= 1. \end{aligned}$$

There are two curves of equilibria passing through the bifurcation point: $x^* = 0$ and $x^* = \mu$. Figure 1.6 shows the stability types of the curves of equilibria.

Definition 1.3.4 *A bifurcation is said to be the supercritical (subcritical) flip bifurcation if a stable steady state becomes unstable and a stable (unstable) period-two solution appears. For a flip bifurcation, we necessarily have* $\lambda = -1$.

Example 1.3.5 Consider the logistic map

$$x_{t+1} = f(x_t, r) = r x_t (1 - x_t). \tag{1.3.8}$$

We can verify that $(x^*, r) = (\frac{2}{3}, 3)$ is an equilibrium with eigenvalue -1, i.e.,

$$\begin{aligned} f(\frac{2}{3}, 3) &= \frac{2}{3}, \\ \frac{\partial f}{\partial x_t}(\frac{2}{3}, 3) &= -1. \end{aligned}$$

Figure 1.7 displays the orbit diagram.

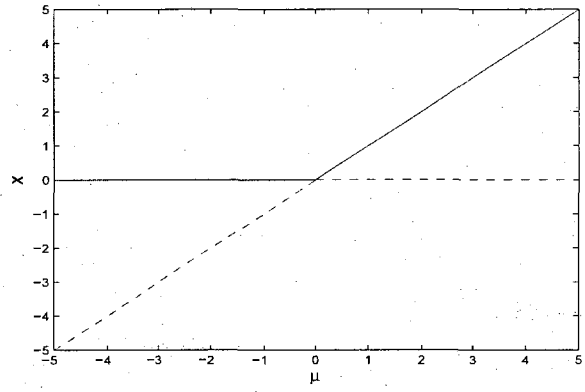

Figure 1.6: Two curves of equilibria pass through the origin. For $\mu < 0$, $x^* = 0$ is stable (solid line) and $x^* = \mu$ is unstable (dashed line). For $\mu > 0$, $x^* = 0$ is unstable (dashed line) and $x^* = \mu$ is stable (solid line).

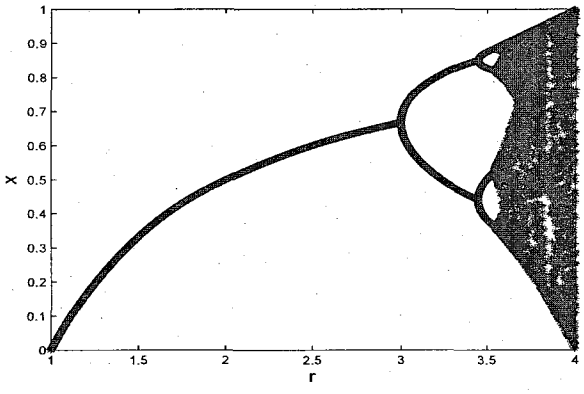

Figure 1.7: For $0 < r < 3$, the equilibrium is stable. At $r = 3$, we observe the first period doubling bifurcation.

Definition 1.3.6 *A bifurcation is said to be the Neimark-Sacker (Hopf) bifurcation if an equilibrium loses stability, the system has periodic solutions, but the period may not be integer valued. For a Neimark-Sacker bifurcation, we necessarily have* $|\lambda| = 1$, $\lambda \notin R$

Jury Conditions

Jury conditions provide a simple way to determine the stability of an equilibrium without knowing the exact eigenvalues. Consider the characteristic equation (1.3.6) where $P(\lambda)$ is a concave-up parabola. If the equation has two real roots, for a stable equilibrium, these two roots must be in the interval $-1 < \lambda < 1$. Equivalently,

$$P(-1) > 0 \tag{1.3.9}$$

and

$$P(+1) > 0. \tag{1.3.10}$$

If the roots are complex conjugates, the absolute value of the root can be written as

$$|\lambda| = \sqrt{\lambda\bar{\lambda}} = \sqrt{\det(J)}. \tag{1.3.11}$$

Hence, for a stable equilibrium,

$$\det(J) < 1. \tag{1.3.12}$$

Inequalities (1.3.9), (1.3.10), and (1.3.12) consitute the Jury test for (1.3.6). Jury conditions are necessary and sufficient to conclude the stability of equilibrium. Since the coefficients of the characteristic equation, i.e. the trace and determinant of the Jacobian matrix, contain the parameters in the model, these inequalities can be applied to find the stability region influenced by the parameters.

In addition, if $P(1) = 0$, then $\lambda = 1$ is an eigenvalue and hence we expect a transcritical bifurcation with the condition that the number of steady states is

not changed. If $P(-1) = 0$, then $\lambda = -1$ is an eigenvalue and we expect a flip bifurcation. If $\det(J) = 1$, then $|\lambda| = 1$ is an eigenvalue and we expect a Neimark-Sacker bifurcation with the condition that the period of limit cycle is nonresonant.

Nicholson-Bailey Model

The Nicholson-Bailey model (Chapter 4 in [22]), which was developed to describe host-parasitoid systems with non-overlapping generations, is in the form of general consumer-resource model. Nicholson and Bailey assume that hosts (F) and parasitoids (C) meet at random and only the first encounter is significant. The standard Nicholson-Bailey model is

$$F_{t+1} = rF_t e^{-aC_t}, \tag{1.3.13}$$

$$C_{t+1} = F_t(1 - e^{-aC_t}), \tag{1.3.14}$$

where r is the host reproductive rate. Both hosts and parasitoids are not considered to clump at any location so the negative exponential function is introduced to represent the probability for parasiotids escaping from parasitoism.

This model has a coexistence equilibrium

$$F^* = \frac{r\ln(r)}{(r-1)a}, \tag{1.3.15}$$

$$C^* = \frac{\ln(r)}{a}. \tag{1.3.16}$$

By applying the Jury conditions on the corresponing Jacobian

$$J = \begin{bmatrix} 1 & -\frac{r\ln(r)}{r-1} \\ \frac{r-1}{r} & \frac{\ln(r)}{r-1} \end{bmatrix} \tag{1.3.17}$$

and the charactieristic polynomial

$$P(\lambda) = \lambda^2 - \left(1 + \frac{\ln(r)}{r-1}\right)\lambda + \frac{\ln(r)r}{r-1}, \tag{1.3.18}$$

we know that $P(-1) > 0$ and $P(+1) > 0$. However, $\det(J) = \frac{\ln(r)r}{r-1} > 1$ for all $r > 1$. Hence, this equilibrium is unstable; small deviations of either hosts or parasitoids from the equilibrium level lead to diverging oscillations. Both populations eventually get very close to zero due to diverging oscillations. Consequently, hosts and parasitoids will be extinct in the real world [2]. Later modifications attempted to stablize the Nicholson-Bailey model by adding new elements or changing some functions. For example, May [20] applied the negative binomial probability function with a stronger aggreation degree instead of negative exponential function to make the Nicholson-Bailey model stable.

Lemma 1.3.7 *The modified Nicholson-Bailey Model*

$$F_{t+1} = rF_t\left(1+\frac{a_F C}{m}\right)^{-m}, \tag{1.3.19}$$

$$C_{t+1} = F_t\left[1-\left(1+\frac{a_F C}{m}\right)^{-m}\right], \tag{1.3.20}$$

is stable for all $m < 1$.

Proof: This system has a coexistence steady state

$$F^* = \frac{mr}{a(r-1)}\left(r^{\frac{1}{m}}-1\right),\ C^* = \frac{m}{a}\left(r^{\frac{1}{m}}-1\right),$$

with the corresponding Jacobian matrix

$$J = \begin{bmatrix} 1 & -\frac{rm}{r-1}\left(1-r^{-\frac{1}{m}}\right) \\ \frac{r-1}{r} & \left(1-r^{-\frac{1}{m}}\right) \end{bmatrix}.$$

To determine its stability, we apply the Jury test to the characteristic polynomial

$$P(\lambda) = \lambda^2 - \left[1+\frac{m}{r-1}\left(1-r^{-\frac{1}{m}}\right)\right]\lambda + \frac{mr}{r-1}\left(1-r^{-\frac{1}{m}}\right).$$

Since

$$P(-1) = 1+1+\frac{m}{r-1}\left(1-r^{-\frac{1}{m}}\right)+\frac{mr}{r-1}\left(1-r^{-\frac{1}{m}}\right) > 0,$$

$$\begin{aligned} P(1) &= 1 - 1 - \frac{m}{r-1}\left(1 - r^{-\frac{1}{m}}\right) + \frac{mr}{r-1}\left(1 - r^{-\frac{1}{m}}\right) \\ &= 1 - r^{-\frac{1}{m}} > 0, \end{aligned}$$

the stability condition reduces to

$$det(J) = g(m) = \frac{mr}{r-1}\left(1 - r^{-\frac{1}{m}}\right) < 1. \tag{1.3.21}$$

Since $g(m) = 1$ at $m = 1$ and $g'(m) > 0$ for all m, we know the condition (1.3.21) is satisfied if $m < 1$. ∎

1.4 Consumer-Resource Model

In this section, we present the main model for this thesis. We follow the approach by Fagan et al [9] of a consumer-resource model of central place foragers. We summarize some of their results and outline the scope of this thesis.

Fagan et al [9] used F_t and C_t to denote the density of resources and consumers at year t, respectively. Resources grow according to the Beverton-Holt growth dynamics $G(F_t)$ and are consumed with a negative exponential probability $p(C_t)$ during the foraging season. Thus, the density of resources at year $t+1$ is $G(F_t)[1 - p(C_t)]$ and the resource consumed during year t is $G(F_t)p(C_t)$. Furthermore, they assumed that consumers breeding is a linearly increasing function of resources consumed and consumers survive from one year to the next with probability s. Hence, the density of consumers at year $t+1$ is $sC_t + \tilde{b}G(F_t)p(C_t)$. Now we introduce space explicitly into the model. We consider a habitat patch of size L with the central location in the middle of the patch. The resource is spatially distributed, which we indicate by writing $F_t(x)$. The distribution of foragers on the patch is given by $k(x)$. The total amount of resource consumed is then given by the integral $\int G(F_t(x))p(C_t k(x))dx$.

Then the spatial consumer-resource model is

$$F_{t+1}(x) = \frac{rKF_t(x)}{K+(r-1)F_t(x)}e^{-a_F C_t k(x)} \tag{1.4.1}$$

$$C_{t+1} = sC_t + \tilde{b}\int_{-L/2}^{L/2} \frac{rKF_t(x)}{K+(r-1)F_t(x)}\left(1-e^{-a_F C_t k(x)}\right)dx. \tag{1.4.2}$$

The foraging distribution (kernel) $k(x)$ is symmetric with the centre at $x=0$ and it's integral over the habitat is less than or equal to one because some individuals might move out the habitat and acquire no food. We assume, however, that all individuals return to the central place.

Fagan et al [9] applied different kinds of foraging kernel $k(x)$ to the model and linearized equation (1.4.2) at the steady state ($F^*=1, C^*=0$) to yield the persistence condition for the consumer,

$$\int_{-L/2}^{L/2} k(x)dx > \frac{(1-s)(K+r-1)}{\tilde{b}Ka_F r}. \tag{1.4.3}$$

The critical patch size L^* for the consumer to persist is given when equation (1.4.3) is an equality. Since the integral of $k(x)$ does not exceed 1, the consumer density cannot persist if $s+\frac{\tilde{b}Ka_F r}{K+r-1}<1$

In addition, they also found that different foraging patch sizes and foraging kernels have different effects on the population dynamics of the consumer. The consumer's equilibrium density increases as the patch size increases; however, increasing patch size might result in instability of the system depending on the foraging kernel. Besides the patch size, the values of other parameters also influence the stability of the model. They plotted stability boundaries for the uniform, tent, and Laplace kernels. Bifurcations occur at different values of parameters for different foraging kernels. For instance, at fixed $L=1.8$, $r=\ln(3)$, $s=0.3$, a bifurcation occurs at $\beta=2.2$ for uniform kernel; $\beta=5.8$ for tent kernel; and $\beta=12.4$ for Laplace kernel.

The foraging kernels mentioned above are constant over time despite individual consumers' foraging decision, which might depend on the distribution of resources.

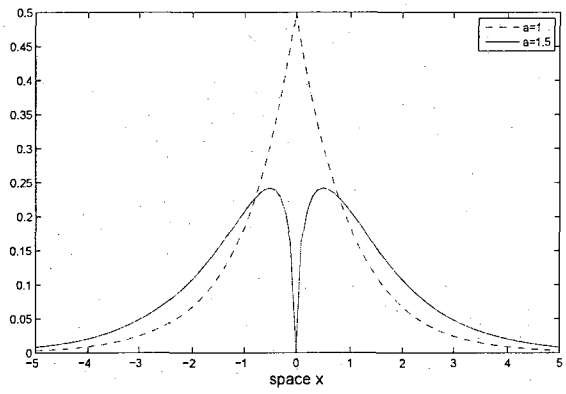

Figure 1.8: Adaptive kernels with $a = 1, 1.5$

Fagan et al [9] introduced a family of foraging kernels with a single parameter. At each time step, they considered the scaled resource distribution F_t and chose the parameter of the kernel to optimize food intake at the population level. More specifically, given $F_t(x)$, they choose $k_t(x)$ from a one-parameter family of kernels as to maximize $\int G(F_t(x))p(C_t k_t(x))dx$. By using this parameter value and the resulting kernel, they obtain the resource distribution and consumer density for the next time step. One of their examples is applying the gamma kernel

$$k_a(x) = \frac{|x|^{a-1}e^{-a|x|}}{2\Gamma(a)}, \tag{1.4.4}$$

with variance $a(a+1)$. Note that this kernel is the Laplace kernel if $a = 1$ and the kernel has peaks away from the central place for $a > 1$ (Figure 1.8).

At each time step, a is modified according to the resource distribution. Figure 1.9 illustrates the foraging kernels at three different time steps.

Like fixed foraging kernels, bifucations can still be found depending on the values of parameters. For instance, a Hopf bifurcation occurs when $\tilde{b}$ is sufficiently large.

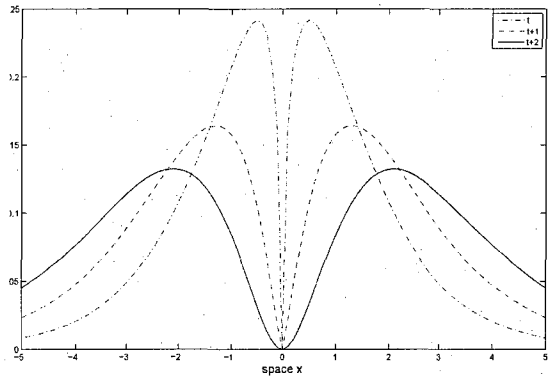

Figure 1.9: Adaptive kernels at different time steps

1.5 Thesis Overview and Notation

We introduce an additional fact that resources obtained farther away from the central place require greater energy to acquire and to transport back to the central place. Hence, there should be a discounting mechanism for the foraging distance. We denote the reduction in energy from a resource item at location x by $R(x)$ and the modified consumer-resource model is given by

$$F_{t+1}(x) = G(F_t(x))(1 - p(C_t k(x))), \tag{1.5.1}$$

$$C_{t+1} = sC_t + \tilde{b}\int_{-L/2}^{L/2} G(F_t(x))p(C_t k(x))R(x)dx, \tag{1.5.2}$$

where the function $R(x)$ is a non-increasing function of distance to the central location. For example, we may define $R(x)$ by

$$R(x) = e^{-a_R|x|}. \tag{1.5.3}$$

More importantly, we consider the case that the resource density influences the consumer foraging behavior. Then the kernel $k(x)$ depends on time. We develop an individual movement model to derive $k_t(x)$ from a given set of rules in Chapter 4.

In Chapter 2 we consider the consumer-resource model in its non-spatial form by assuming the foraging kernel is uniform. We apply the Beverton-Holt, Holling Type 1, and Logistic growth funtions for G as well as the negative exponential and negative binomial functions for p to the model. We nondimensionalize each model with the same nondimensional quantities to reduce the number of parameters. Next, we find the equilibria and corresponding Jacobian matrices and characteristic polynomials. Then we determine the stability region for each equilibrium. In the case that there is no explicit formula for an equilibrium, we determine the steady state numerically. In addition, we explore the effects of parameters on a steady state's behavior by varing one parameter and fixing other parameters at a time, i.e. we produce one-dimensional bifurcation diagrams.

In Chapter 3, the model is now spatially explicit with the foraging kernel being fixed in time. Following Fagan et al [9], we choose the Laplace kernel. We focus on the compensatory dynamics by applying the Beverton-Holt growth function for G. We consider two cases: random search (negative exponential) and clumped search (negative binomial) by consumers. We calculate an implicit formula for the coexistence steady state and find the domain where resources at the steady state are completely depleted. We simulate the system and apply the same technique (vary one parameter and fix others) to investigate the effects of parameters. We find the stable region and generate the bifurcation diagram for each parameter.

In Chapter 4 we apply a random-walk framework to derive the foraging kernel $k(x)$ based on individual movement rules. We assume that consumers move randomly in space until they settle at some location to forage. This approach leads to a system of PDEs, more specifically a diffusion equation for moving individuals coupled to an ordinary differential equation for settled individuals. We first consider that the settling rate is a constant. We solved the resulting PDEs with the initial conditions that all individuals are at the central place at the beginging and settle to forage before the foraging season ends. The foraging kernel $k(x)$ is the distribution of settled

consumers. We find that $k(x)$ is in fact the Laplace kernel for the constant settling rate. Next, we consider that the consumer's decision on whether to settle depends on the abundance of resource. We introduce the Hill function as the non-decreasing function of settling rate. We assume the resource is fixed and consider three cases: (1) the resource is homogeneous; (2) the resource is low near the central location; and (3) the resource is depleted completely near the central place. We investigate how the paramters in the Hill function affect the shape of foraging kernel. We find that the foraging kernel might have a single peak at the central location or two peaks at equal distance from the centre. We also determine the mean and variance of the kernel.

In Chapter 5, we apply the resource-dependent foraging kernel to our consumer-resource model. The analysis in the chapter is mainly based on numerical simulations. We study the population dynamics by varying each parameter individually. As in the previous cases, we find that the model with resource-dependent kernel can exhibit a stable coexistence steady state or consumer-resource cycles. We illustrate various resource-dependent kernels over the course of one such cycle. We also plot bifurcation diagrams for each parameter to illustrate the effect of different foraging mechanisms on population dynamics. Comparing the model with resource-dependent kernel to the one with fixed Laplace kernel, we find that the qualitative behavior is very similar in many cases. However, in some cases, the qualitative behavior of two models is markedly different.

Chapter 2

Non-Spatial Dynamics

In this section, we assume that consumers distribute evenly in the domain to forage, i.e., $k_t(x) = k(x)$ is a constant for the uniform foraging kernel. We consider $k(x) = \frac{1}{L}$ such that $\int_{-L/2}^{L/2} k(x)dx = 1$. Furthermore, we assume that $F_0(x) = 1$ is constant in space. Then $F_t(x)$ is also a constant in space for all t and $\int R(x)dx$ turns into a factor scaling $\tilde{b}$. Hence, the consumer-resource model reduces to the non-spatial model in the form of

$$F_{t+1} = G(F_t)\left[1 - p\left(\frac{C_t}{L}\right)\right], \tag{2.0.1}$$

$$C_{t+1} = sC_t + L\tilde{b}G(F_t)p\left(\frac{C_t}{L}\right). \tag{2.0.2}$$

We start the analysis of this non-spatial consumer-resource model by introducing the nondimensional quantities $F_t = Kf_t$, $C_t = \frac{L}{a_F}c_t$, and $\tilde{b} = \frac{1}{a_F K}b$. Nondimensionalization allows us to focus on the effects of parameters r, s, and b upon the stability of equilibria by eliminating other parameters. Next, we find the equilibria from the nondimensionalized model and determine their stability region. We compute the Jacobian matrix for each equilibrium. Then we apply the Jury test to the corresponding characteristic polynomial to verify whether the equilibrium is stable, to find the conditions for an equilibrium to be stable, and to justify the type of bifurcation when

the equilibrium becomes unstable.

2.1 Compensatory Dynamics

We consider the Beverton-Holt and Holling Type 1 functions as the resource growth function G, and negative exponential and negative binomial with aggregation degree one functions as the probability function p for resources being consumed successfully.

2.1.1 Beverton-Holt Dynamics and Negative Exponential Probability

We start by applying Beverton-Holt growth function coupled with negative exponential probability function. Then we obtain the following two-dimensional system:

$$F_{t+1} = \frac{rKF_t}{K+(r-1)F_t}\exp\left(\frac{-a_F C_t}{L}\right), \tag{2.1.1}$$

$$C_{t+1} = sC_t + L\tilde{b}\frac{rKF_t}{K+(r-1)F_t}\left[1-\exp\left(\frac{-a_F C_t}{L}\right)\right]. \tag{2.1.2}$$

With the nondimensional quantities, we rewrite (2.1.1) and (2.1.2) as

$$f_{t+1} = \frac{rf_t}{1+(r-1)f_t}\exp\left(-c_t\right), \tag{2.1.3}$$

$$c_{t+1} = sc_t + \frac{brf_t}{1+(r-1)f_t}\left[1-\exp\left(-c_t\right)\right]. \tag{2.1.4}$$

There are three equilibria for this system: the equilibrium $(0,0)$, the semi-trivial equilibrium $(1,0)$, and the coexistence equilibrium.

This coexistence equilibrium cannot be expressed in terms of s, r, b explicitly. However, from (2.1.3) and (2.1.4), we have

$$f^* = \frac{rf^*}{1+(r-1)f^*}e^{-c^*},$$

$$c^* = sc^* + \frac{brf^*}{1+(r-1)f^*}\left(1-e^{-c^*}\right).$$

That is,

$$\begin{aligned} f^* &= \frac{re^{-c^*}-1}{r-1}, \\ c^* &= \frac{brf^*}{(1-s)[1+(r-1)f^*]}\left(1-e^{-c^*}\right) \\ &= \frac{b}{1-s}f^*\left(e^{c^*}-1\right). \end{aligned}$$

Thus, we have the implicit coexistence equilibrium

$$f^* = \frac{re^{-c^*}-1}{r-1} = \frac{(1-s)c^*}{b(e^{c^*}-1)},\ c^* = \frac{b}{(1-s)(r-1)}(r+1-e^{c^*}-re^{-c^*}). \quad (2.1.5)$$

We note that this coexistence equilibrium is biologically meaningful only if $r > 1$ and $r > e^{c^*}$. In addition, the following lemma shows that the condition $s + b > 1$ is necessary for the system to have a unique coexistence steady state.

Lemma 2.1.1 *The coexistence equilibrium exists if $s + b > 1$ and it is unique.*

Proof: Suppose the consumer density $c > 0$. Let $h(c) = c$ and

$$g(c) = \frac{b}{(1-s)(r-1)}(r+1-e^c-re^{-c}).$$

Since $g'(c) = \frac{b}{(1-s)(r-1)}(-e^c+re^{-c})$, we have $g'(0) = \frac{b}{1-s} > 1$ for $s+b > 1$. Next, $g''(c) = \frac{b}{(1-s)(r-1)}(-e^c-re^{-c}) < 0$ implies that $g(c)$ has one maximum at $c = \ln(\sqrt{r})$. Hence, there is only one intersection between $h(c)$ and $g(c)$ for $c > 0$, and this equilibrium is unique. ∎

Linearizing equations (2.1.3) and (2.1.4) yields the Jacobian matrix:

$$J(f,c) = \begin{bmatrix} \frac{re^{-c}}{[1+(r-1)f]^2} & \frac{-rfe^{-c}}{1+(r-1)f} \\ \frac{br(1-e^{-c})}{[1+(r-1)f]^2} & s+\frac{brfe^{-c}}{1+(r-1)f} \end{bmatrix}. \quad (2.1.6)$$

At the trivial steady state, we obtain

$$J(0,0) = \begin{bmatrix} r & 0 \\ 0 & s \end{bmatrix}. \tag{2.1.7}$$

Since $0 < s < 1$ by definition, the trivial equilibrium is thus unstable for $r > 1$.

Moreover, at the semi-trivial steady state (exists only when $r > 1$), the Jacobian matrix is given by

$$J(1,0) = \begin{bmatrix} \frac{1}{r} & -1 \\ 0 & s+b \end{bmatrix}. \tag{2.1.8}$$

Thus, the semi-trivial equilibrium is stable if $r > 1$ and $s + b < 1$.

At the coexistence equilibrium, the Jacobian matrix is

$$J(f^*, c^*) = \begin{bmatrix} \frac{e^c}{r} & -\frac{re^{-c}-1}{r-1} \\ \frac{b(e^{2c}-e^c)}{r} & s + \frac{b(re^{-c}-1)}{r-1} \end{bmatrix}. \tag{2.1.9}$$

Lemma 2.1.2 *The coexistence equilibrium is stable if*

$$\frac{se^c}{r} + \frac{be^{2c}(re^{-c}-1)}{r(r-1)} < 1, \tag{2.1.10}$$

where c is the consumer density at the coexistence equilibrium.

Proof: The Jacobian matrix (2.1.9) has the characteristic polynomial:

$$\begin{aligned} P(\lambda) &= \lambda^2 - a_1\lambda + a_2 \\ &= \lambda^2 - \left[\frac{e^c}{r} + s + \frac{b(re^{-c}-1)}{r-1}\right]\lambda + \left[\frac{se^c}{r} + \frac{b(re^c - e^{2c})}{r(r-1)}\right]. \end{aligned} \tag{2.1.11}$$

By applying the Jury test to (2.1.11), we have

$$P(-1) = 1 + \frac{e^c}{r} + s + \frac{b(re^{-c}-1)}{r-1} + \frac{se^c}{r} + \frac{b(re^c - e^{2c})}{r(r-1)}, \tag{2.1.12}$$

$$P(1) = 1 - \frac{e^c}{r} - s - \frac{b(re^{-c}-1)}{r-1} + \frac{se^c}{r} + \frac{b(re^c - e^{2c})}{r(r-1)}, \tag{2.1.13}$$

$$a_2 = \frac{se^c}{r} + \frac{b(re^c - e^{2c})}{r(r-1)}. \tag{2.1.14}$$

The expression (2.1.12) is clearly greater than zero. Furthermore, the expression (2.1.13) is also greater than zero since

$$\begin{aligned}
P(1) &= 1 - \frac{e^c}{r} - s - \frac{b(re^{-c}-1)}{r-1} + \frac{se^c}{r} + \frac{b(re^c - e^{2c})}{r(r-1)} \\
&= (1-s) - \frac{e^c}{r}(1-s) - \frac{b(re^{-c}-1)}{r-1}\left(1 - \frac{e^{2c}}{r}\right) \\
&= (1-s)\left(1 - \frac{e^c}{r}\right) - \frac{b(re^{-c}-1)}{r-1}\left(1 - \frac{e^{2c}}{r}\right) \\
&\geq (1-s)\left(1 - \frac{e^c}{r}\right) - \frac{b(re^{-c}-1)}{r-1}\left(1 - \frac{e^c}{r}\right) \\
&= \left(1 - \frac{e^c}{r}\right)\left(1 - s - \frac{b(re^{-c}-1)}{r-1}\right) \\
&= \left(1 - \frac{e^c}{r}\right)(1 - s - bf) \\
&= \left(1 - \frac{e^c}{r}\right)\left(1 - s - b\frac{(1-s)c}{b(e^c-1)}\right) \\
&= \left(1 - \frac{e^c}{r}\right)(1-s)\left(\frac{c}{e^c-1}\right) > 0,
\end{aligned}$$

where $\frac{c}{e^c-1} > 0$ for $c > 0$. Hence, the stability condition is reduced to

$$\frac{se^c}{r} + \frac{be^{2c}(re^{-c}-1)}{r(r-1)} < 1. \tag{2.1.15}$$

∎

We observe that both resource and consumer populations oscillate with constant amplitudes when (2.1.10) is not satisfied. Figure 2.1 shows both densities for t between 2000 and 2300.

There are three parameters in the non-dimensionalized non-spatial model. To explore the effects of each parameter on the stability of equilibria, we solve both

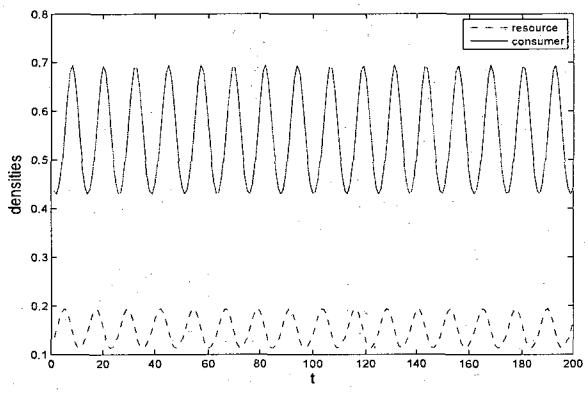

Figure 2.1: The densities of resource and consumer after 2000 generations where $s = 0.5$, $b = 4$, $r = 2$, $a_2 = 4.25e^c - 2e^{2c}$. The condition (2.1.10) is not satisfied. Both populations oscillate with constant amplitudes.

resource and consumer populations numerically for the last 35 generations of 5000 generations. Formula (2.1.5) shows that c^* is increasing with s and with b (fixed r). Equation (2.1.14) shows that a_2 is also increasing with s and b. Hence, for fixed b and r, we expect a Neimark-Sacker bifurcation as s increases. Similarly for fixed s and r, and varing b. The influence of r is not clear from the formula but we can observe that the consumer density oscillates for a smaller value of r in Figure 2.3.

Figure 2.2, Figure 2.3, and Fig 2.4 show that bifurcations occur for various values of s, r, and b, respectively.

The density of consumers increases significantly if they have higher survival rate or higher conversion coefficient. From the above figures, we observe that larger s or b leads the equilibrium to an oscillation. We also find that smaller r causes the equilibrium to be unstable. Figure 2.5 shows the stability region with respect to b and r at $s = 0.2, 0.5$. Limit cycles are found for the values to the right of the line.

If $r < 1$, both resource and consumer in the system will go extinct. If $r > 1$ but $s + b < 1$, the consumer cannot persist and the system reaches the equilibrium at which only resource exists. If $r > 1$ and $s + b > 1$, resources and consumers coexist

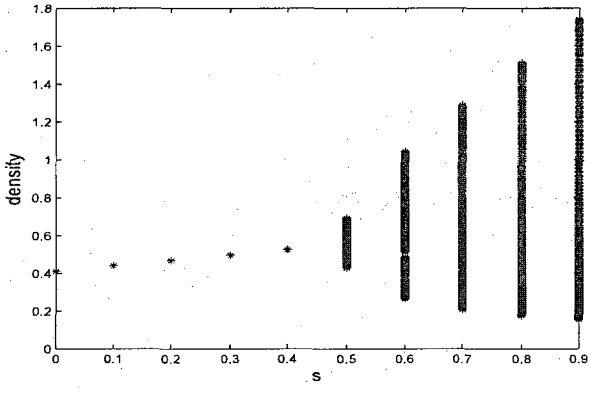

Figure 2.2: Bifurcation of model (2.1.3), (2.1.4) for increasing s with fixed $r = 2$, $b = 2.5$. A Neimark-Sacker bifurcation is observed as s increases.

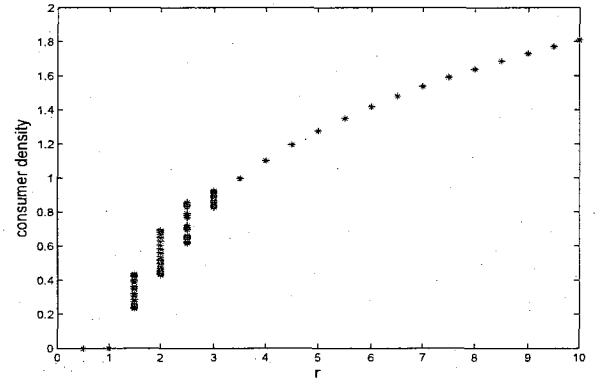

Figure 2.3: Bifurcation of model (2.1.3), (2.1.4) for increasing r with fixed $s = 0.5$, $b = 2.5$. A Neimark-Sacker bifurcation is observed as r decreases.

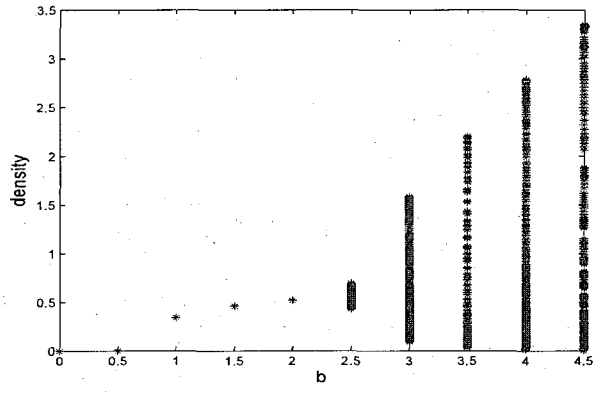

Figure 2.4: Bifurcation of model (2.1.3), (2.1.4) for increasing b with fixed $s = 0.5$, $r = 2$. A Neimark-Sacker bifurcation is observed as b increases.

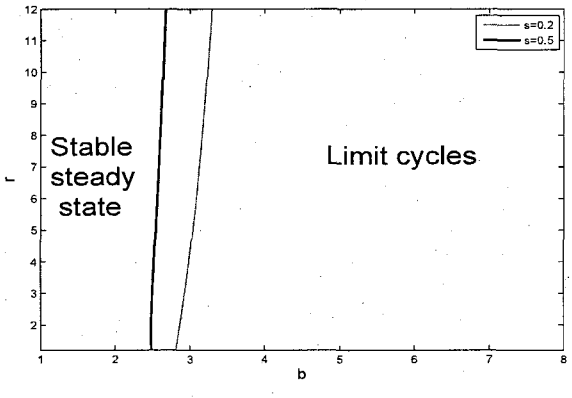

Figure 2.5: Stable and unstable region of model (2.1.3), (2.1.4) for $s = 0.2, 0.5$.

and the stability depends on the condition indicated in Lemma 2.1.2.

2.1.2 Beverton-Holt Dynamics and Negative Binomial Probability

The Nicholson-Bailey model becomes stable if a clumped search by parasitoids is considered. In this section, we consider the compensatory dynamic described by the Beverton-Holt growth function coupled with the negative binomial probability function. The resulting equations are:

$$F_{t+1} = \frac{rKF_t}{K+(r-1)F_t}\left(\frac{1}{1+\frac{a_F C_t}{L}}\right), \tag{2.1.16}$$

$$C_{t+1} = sC_t + L\tilde{b}\frac{rKF_t}{K+(r-1)F_t}\left(1-\frac{1}{1+\frac{a_F C_t}{L}}\right). \tag{2.1.17}$$

By introducing nondimensional quantities, we rewrite equations (2.1.16) and (2.1.17) as:

$$f_{t+1} = \frac{rf_t}{1+(r-1)f_t}\left(\frac{1}{1+c_t}\right), \tag{2.1.18}$$

$$c_{t+1} = sc_t + \frac{brf_t}{1+(r-1)f_t}\left(\frac{c_t}{1+c_t}\right). \tag{2.1.19}$$

This system has three equilibria: the trivial equilibrium $(0,0)$, the semi-trivial equilibrium $(1,0)$, and the coexistence equilibrium

$$f^* = \frac{1-s}{b},\ c^* = \frac{(r-1)(b-1+s)}{b+(1-s)(r-1)}. \tag{2.1.20}$$

This coexistence equilibrium is biologically meaningful if $r>1$ and $s+b>1$. We linearize equations (2.1.18) and (2.1.19) with respect to f and c. Then we obtain the Jacobian matrix:

$$J(f,c) = \begin{bmatrix} \frac{r}{[1+(r-1)f]^2}\frac{1}{1+c} & \frac{-rf}{1+(r-1)f}\frac{1}{(1+c)^2} \\ \frac{br}{[1+(r-1)f]^2}\frac{c}{1+c} & s+\frac{brf}{1+(r-1)f}\frac{1}{(1+c)^2} \end{bmatrix}. \tag{2.1.21}$$

At the trivial equilibrium, we have

$$J(0,0) = \begin{bmatrix} r & 0 \\ 0 & s \end{bmatrix}. \tag{2.1.22}$$

The eigenvalues are r and s. The trivial equilibrium is thus unstable for $r > 1$.

At the semi-trivial equilibrium, the Jacobian matrix is given by

$$J(1,0) = \begin{bmatrix} \frac{1}{r} & -1 \\ 0 & s+b \end{bmatrix}. \tag{2.1.23}$$

The eigenvalues are $\frac{1}{r}$ and $s+b$. Therefore, the semi-trivial equilibrium is stable for $r > 1$ and $s + b < 1$.

At the coexistence equilibrium, the Jacobian matrix is given by

$$J(f^*, c^*) = \begin{bmatrix} \frac{b}{b+(r-1)(1-s)} & \frac{-(1-s)[b+(r-1)(1-s)]}{b^2 r} \\ \frac{b^2(r-1)(b-1+s)}{[b+(r-1)(1-s)]^2} & s + \frac{(1-s)[b+(r-1)(1-s)]}{br} \end{bmatrix}. \tag{2.1.24}$$

Lemma 2.1.3 *The coexistence equilibrium is stable for $r > 1$, $s + b > 1$.*

Proof: The characteristic polynomial of Jacobian matrix (2.1.24) is

$$\begin{aligned} P(\lambda) &= \lambda^2 - a_1\lambda + a_2 \\ &= \lambda^2 - \left[s + \frac{b^2 r + (1-s)[b+(r-1)(1-s)]^2}{br[b+(r-1)(1-s)]}\right]\lambda + 1 - \frac{b}{b+(r-1)(1-s)}. \end{aligned}$$

According to the Jury test, the stability conditions for the coexistence equilibrium are

$$P(-1) = 1 + \left[s + \frac{b^2 r + (1-s)[b+(r-1)(1-s)]^2}{br[b+(r-1)(1-s)]}\right] + 1 - \frac{b}{b+(r-1)(1-s)} > 0, \tag{2.1.25}$$

$$P(1) = 1 - \left[s + \frac{b^2 r + (1-s)[b+(r-1)(1-s)]^2}{br[b+(r-1)(1-s)]}\right] + 1 - \frac{b}{b+(r-1)(1-s)} > 0, \tag{2.1.26}$$

and

$$a_2 = 1 - \frac{b}{b + (r-1)(1-s)} < 1. \tag{2.1.27}$$

Then the inequalities (2.1.25), (2.1.26), and (2.1.27) can be reduced to

$$1 + s + \frac{2b^2 r + (1-s)[b + (r-1)(1-s)]^2}{br[b + (r-1)(1-s)]} > 0, \tag{2.1.28}$$

$$1 - s + \frac{(1-s)[b + (r-1)(1-s)]^2}{br[b + (r-1)(1-s)]} > 0, \tag{2.1.29}$$

and

$$\frac{b}{b + (r-1)(1-s)} < 1. \tag{2.1.30}$$

respectively. Since $r > 1$ and $s + b > 1$ for a biologically meaningful coexistence equilibrium, conditions (2.1.28), (2.1.29), and (2.1.30) are all satisfied. Hence, the coexistence equilibrium is stable. ∎

By comparing to the model in the previous subsection, we find that the negative binomial function stablizes the non-spatial model with Beverton-Holt growth function. The model always converges to an equilibrium for all s, r, and b. Figure 2.6 illustrates that the consumer density is stable at the coexistence steady state for all s. Also, from (2.1.20), we expect the consumer density increases but the resource density decreases as s increases. Similarly to the other parameters, both resource and consumer density converge to equilibria for all r and b. Note that the coexistence state value of the resource population is independent of r.

If $r < 1$, the trivial equilibrium is stable and both resources and consumers go extinct eventually. If $r > 1$ but $s + b < 1$, the trivial equilibrium becomes unstable and the semi-trivial equilibrium is stable. In this case, the consumer goes extinct but the resource persists in the system. If $r > 1$ and $s + b > 1$, only the coexistence equilibrium is stable. The resource and consumer can coexist in the system with stable populations.

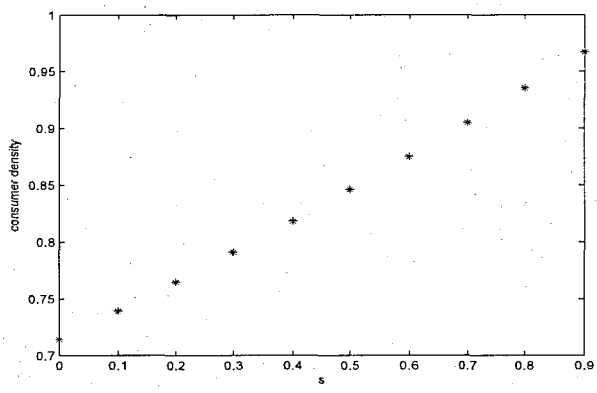

Figure 2.6: Consumer populations of model (2.1.18), (2.1.19) for increasing s with fixed $b = 6$, $r = 2$. The consumer density converges to a stable steady state for all values of s.

2.1.3 Holling Type 1 Dynamics and Negative Exponential Probability

In this section, we apply Holling Type 1 function instead of Beverton-Holt function as the resource growth function. We first consider the negative exponential function for the probability of resource being consumed successfully. The resulting equations are:

$$F_{t+1} = rF_t \exp\left(\frac{-aC_t}{L}\right), \tag{2.1.31}$$

$$C_{t+1} = sC_t + L\tilde{b}rF_t\left[1 - \exp\left(\frac{-aC_t}{L}\right)\right], \tag{2.1.32}$$

for $rF \leq K$, and

$$F_{t+1} = K \exp\left(\frac{-a_F C_t}{L}\right), \tag{2.1.33}$$

$$C_{t+1} = sC_t + L\tilde{b}K\left[1 - \exp\left(\frac{-aC_t}{L}\right)\right], \tag{2.1.34}$$

for $rF > K$.

We introduce the same nondimensional quantities and rewrite equations (2.1.31) and (2.1.32) as

$$f_{t+1} = rf_t e^{-c_t}, \tag{2.1.35}$$

$$c_{t+1} = sc_t + brf_t\left(1 - e^{-c_t}\right), \tag{2.1.36}$$

where $rf < 1$, and equations (2.1.33) and (2.1.34) as

$$f_{t+1} = e^{-c_t}, \tag{2.1.37}$$

$$c_{t+1} = sc_t + b\left(1 - e^{-c_t}\right), \tag{2.1.38}$$

where $rf > 1$.

Similarly, we find equilibria for each case then analyze their stability. For the case $rf < 1$, there are two equilibria: the trivial equilibrium $(0, 0)$ and the coexistence equilibrium

$$f^* = \frac{(1-s)\ln(r)}{b(r-1)},\ c^* = \ln(r) \tag{2.1.39}$$

where $r > 1$ for a biologically meaningful consumer density. We note that for the condition $rf^* < 1$ to be satisfied, we require

$$\frac{r\ln(r)}{r-1} < \frac{b}{1-s}. \tag{2.1.40}$$

The corresponding Jacobian matrix is

$$J(f,c) = \begin{bmatrix} re^{-c} & -rfe^{-c} \\ br\left(1-e^{-c}\right) & s + brfe^{-c} \end{bmatrix}. \tag{2.1.41}$$

For the case $rf > 1$, there are also two equilibira: the semi-trivial equilibrium $(1, 0)$ and another coexistence equilibrium (f^*, c^*) where

$$f^* = e^{-c^*} = 1 - \frac{(1-s)c^*}{b}. \tag{2.1.42}$$

Since the slope of e^{-c^*} is $-e^{-c^*} < 0$ and the slope of $1 - \frac{(1-s)c^*}{b}$ is $\frac{-(1-s)}{b} < 0$, a unique intersection exists for $c^* > 0$ if $\frac{-(1-s)}{b} > -1$, i.e. $s + b > 1$. Also, we require

that $c^* < \frac{b}{1-s}$ so that the resource density is biologically meaningful. In addition, since $rf^* > 1$, we need

$$c^* < \frac{(r-1)b}{r(1-s)}. \tag{2.1.43}$$

We then obtain the Jacobian matrix in this case

$$J(f,c) = \begin{bmatrix} 0 & -e^{-c} \\ 0 & s + be^{-c} \end{bmatrix}. \tag{2.1.44}$$

To determine the stability, we apply the corresoponding Jacobian matrix for each equilibrium. At the trivial equilibrium, we have

$$J(0,0) = \begin{bmatrix} r & 0 \\ 0 & s \end{bmatrix}. \tag{2.1.45}$$

The trivial equilibrium is stable if $r < 1$. Likewise, at the semi-trivial equilibrium, the corresponding Jacobian matrix is given by

$$J(1,0) = \begin{bmatrix} 0 & -1 \\ 0 & s+b \end{bmatrix} \tag{2.1.46}$$

The semi-trivial equilibrium is thus stable if $s + b < 1$. Moreover, at the coexistence equilibrium where $rf < 1$, we have the Jacobian matrix

$$J(f^*,c^*) = \begin{bmatrix} 1 & -\frac{(1-s)\ln(r)}{b(r-1)} \\ b(r-1) & s + \frac{(1-s)\ln(r)}{r-1} \end{bmatrix}. \tag{2.1.47}$$

Lemma 2.1.4 *The coexistence equilibrium where $rf^* < 1$ is unstable.*

Proof: The characterisitic polynomial of (2.1.47) is

$$\begin{aligned} P(\lambda) &= \lambda^2 - a_1\lambda + a_2 \\ &= \lambda^2 - \left[1 + s + \frac{(1-s)\ln(r)}{r-1}\right]\lambda + \left[s + (1-s)\ln(r) + \frac{r}{r-1}\right] \end{aligned} \tag{2.1.48}$$

To apply the Jury test, we evaluate

$$P(-1) = 1 + 1 + s + \frac{(1-s)\ln(r)}{r-1} + s + (1-s)\ln(r) + \frac{r}{r-1}, \tag{2.1.49}$$

$$P(1) = 1 - 1 - s - \frac{(1-s)\ln(r)}{r-1} + s + (1-s)\ln(r) + \frac{r}{r-1}, \quad (2.1.50)$$

$$a_2 = s + (1-s)\ln(r) + \frac{r}{r-1}. \quad (2.1.51)$$

Equations (2.1.50) and (2.1.51) can be simplified to

$$P(-1) = 2 + 2s + \frac{r}{r-1}\left[(1-s)\ln(r) + 1\right], \quad (2.1.52)$$

$$P(1) = (1-s)\ln(r)\frac{r-2}{r-1} + \frac{r}{r-1}. \quad (2.1.53)$$

According to the Jury test, the equilibrium is stable if $P(-1) > 0$, $P(1) > 0$, and $a_2 < 1$. However,

$$s + (1-s)\ln(r) > 0 > \frac{-1}{r-1} = 1 - \frac{r}{r-1} \quad (2.1.54)$$

implies that $a_2 > 1$. Hence, the Jury test is not satisfied and this coexistence equilibrium is unstable. ∎

Since the Jacobian matrix at this equilbrium has complex conjugate eigenvalues whose absolute values are greater than one, this equilibrium is unstable and we expect oscillating solutions. Figure 2.7 shows limit cycles for both resource and consumer when $\frac{r\ln(r)}{r-1} < \frac{b}{(1-s)}$.

For the other coexistence steady state where $rf^* > 1$, the Jacobian matrix is given by

$$J(f^*, c^*) = \begin{bmatrix} 0 & -e^{-c^*} \\ 0 & s + be^{-c^*} \end{bmatrix}. \quad (2.1.55)$$

The eigenvalues of this Jacobian matrix are 0 and $s + be^{-c^*}$, which is real and greater than zero.

Lemma 2.1.5 *The coexistence equilibrium where $rf^* > 1$ is stable.*

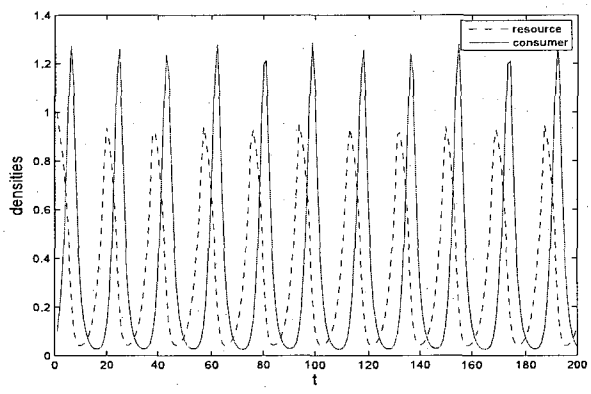

Figure 2.7: At $s = 0.5$, $b = 1.5$, $r = 1.5$, both resource and consumer densities oscillate.

Proof: For the equilibrium to be stable, we need

$$s + be^{-c^*} < 1. \tag{2.1.56}$$

Or equivalently,

$$1 < \frac{1-s}{b} e^{c^*}. \tag{2.1.57}$$

From (2.1.38), we know that $c^* = sc^* + b\left(1 - e^{-c^*}\right)$; i.e. $\frac{1-s}{b} = \frac{1-e^{-c^*}}{c^*}$.

Thus,

$$\frac{1-s}{b} e^{c^*} = \frac{1-e^{-c^*}}{c^*} e^{c^*} = \frac{e^{c^*}-1}{c^*} > 1 \tag{2.1.58}$$

Hence, the coexistence equilibrium is stable. ∎

The parameters in this model have a similar influence on stability as in the model with Beverton-Holt growth function: for the coexistence equilibrium where $rf^* < 1$, smaller r leads both populations to limit cycles but smaller s or b results in a stable equilibrium. Figure 2.8 shows the stable region with respective to b and r for different

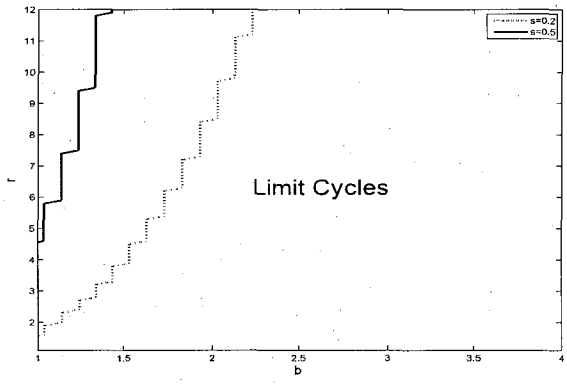

Figure 2.8: Stable and unstable region of model (2.1.35), (2.1.36), (2.1.37), (2.1.38) for $s = 0.2, 0.5$.

values of $s = 0.2, 0.5$. The system has a limit cycle if paramter values fall at the right of line.

Remark 2.1.6 From the previous lemma, we have shown that the coexistence steady state is stable for $rf^* > 1$. We know that c^* increases as b or s increases. Therefore, the condition $rf^* = re^{-c^*} > 1$ is violated for a larger value of b or s, or a smaller value of r. At the point where $re^{-c^*} = 1$, the growth function is not differentiable. Therefore, classical bifurcation theory does not apply. Figure 2.9, Figure 2.10, and Figure 2.11 show the orbits of model (2.1.35), (2.1.36), (2.1.37), (2.1.38) with respect to s, r, and b respectively. These figures illustrate when an oscillation is observed

If $r < 1$, both resource and consumer go extinct. If $r > 1$ but $s + b < 1$, only resources can persist. If r is large enough and $s + b > 1$, the resource and consumer may reach a stable coexistence equilibrium or stable cycles depending on the values of parameters.

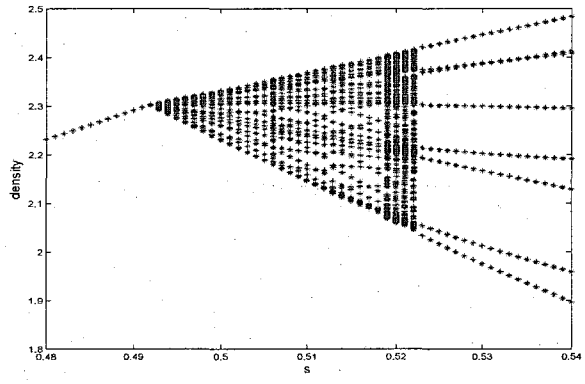

Figure 2.9: Bifurcation of model (2.1.35), (2.1.36), (2.1.37), (2.1.38) for increasing s with fixed $b = 1.3$, $r = 10$. A bifurcation is observed as s increases.

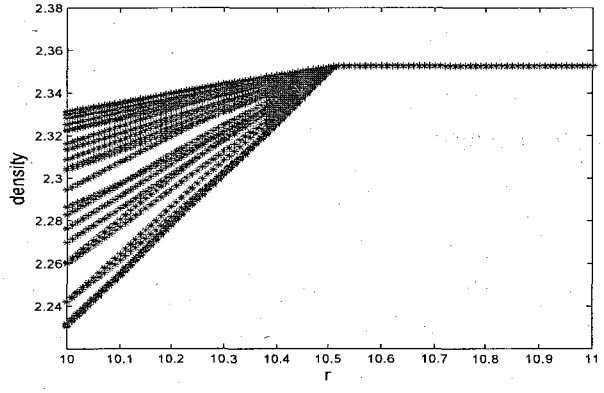

Figure 2.10: Bifurcation of model (2.1.35), (2.1.36), (2.1.37), (2.1.38) for increasing r with fixed $s = 0.5$, $b = 1.3$. A bifurcation is observed as r decreases.

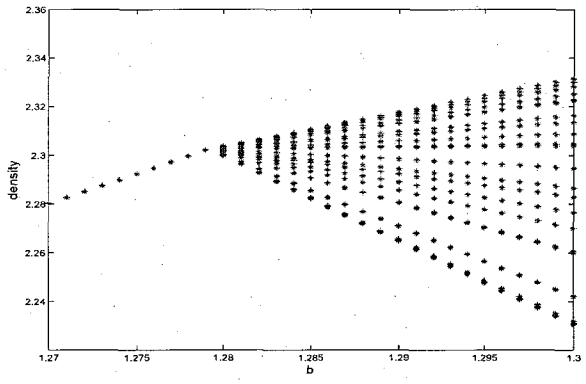

Figure 2.11: Bifurcation of model (2.1.35), (2.1.36), (2.1.37), (2.1.38) for increasing b with fixed $s = 0.5$, $r = 10$. A bifurcation is observed as b increases.

2.1.4 Holling Type 1 Dynamics and Negative Binomial Probability

In this section, we still apply Holling Type 1 function but consider clumped search by consumers as modeled by the negative bionomial probability function. The modified equations are:

$$F_{t+1} = rF_t\left(\frac{1}{1+\frac{aC_t}{L}}\right), \tag{2.1.59}$$

$$C_{t+1} = sC_t + L\tilde{b}rF_t\left(1-\frac{1}{1+\frac{aC_t}{L}}\right), \tag{2.1.60}$$

for $rF \leq K$, and

$$F_{t+1} = \frac{K}{1+\frac{aC_t}{L}}, \tag{2.1.61}$$

$$C_{t+1} = sC_t + L\tilde{b}K\left(1-\frac{1}{1+\frac{aC_t}{L}}\right), \tag{2.1.62}$$

for $rF > K$.

After nondimensionalizing, equations (2.1.59) and (2.1.60) are rewriten as

$$f_{t+1} = \frac{rf_t}{1+c_t}, \tag{2.1.63}$$

$$c_{t+1} = sc_t + \frac{brf_tc_t}{1+c_t}, \tag{2.1.64}$$

for $rf \leq 1$, whereas equations (2.1.61), (2.1.62) are rewriten as

$$f_{t+1} = \frac{1}{1+c_t}, \tag{2.1.65}$$

$$c_{t+1} = sc_t + \frac{bc_t}{1+c_t}, \tag{2.1.66}$$

for $rf > 1$.

For the case $rf \leq 1$, the system of equations (2.1.63) and (2.1.64) has two equilibria: the trivial equilibrium $(0,0)$ and the coexistence equilibrium

$$f^* = \frac{1-s}{b},\ c^* = r-1 \tag{2.1.67}$$

where $r > 1$ is necessary for a biologically meaningful consumer population. The Jacobian matrix in this case is

$$J(f,c) = \begin{bmatrix} \frac{r}{1+c} & \frac{-rf}{(1+c)^2} \\ \frac{brc}{1+c} & s + \frac{brf}{(1+c)^2} \end{bmatrix}. \tag{2.1.68}$$

For the case $rf > 1$, the system of equations (2.1.65) and (2.1.66) also has two equilibria: the semi-trivial equilibrium $(1,0)$ and another coexistence equilibrium

$$f^* = \frac{1-s}{b},\ c^* = \frac{b}{1-s} - 1 \tag{2.1.69}$$

where $s+b > 1$ is necessary for a biologically meaningful consumer density. The Jacobian matrix in this case is

$$J(f,c) = \begin{bmatrix} 0 & \frac{-1}{(1+c)^2} \\ 0 & s + \frac{b}{(1+c)^2} \end{bmatrix}. \tag{2.1.70}$$

Since the coexistence equilibria for the resource ($f^* = \frac{1-s}{b}$) are the same in both cases, we have $rf \leq 1$ if and only if

$$r \leq \frac{b}{1-s}. \tag{2.1.71}$$

Next, we find the Jacobian matrix for each equilibrium. At the trivial equilibrium, we have

$$J(0,0) = \begin{bmatrix} r & 0 \\ 0 & s \end{bmatrix}. \tag{2.1.72}$$

The trivial equilibrium is thus stable for $r < 1$. At the semi-trivial equilibrium, we have

$$J(1,0) = \begin{bmatrix} 0 & -1 \\ 0 & s+b \end{bmatrix}. \tag{2.1.73}$$

The semi-trivial equilibrium is stable if $s + b < 1$. Furthermore, at the coexistence equilibrium where $rf \leq 1$; i.e. $r \leq \frac{b}{1-s}$, the Jacobian matrix is given by

$$J(f^*, c^*) = \begin{bmatrix} 1 & \frac{-(1-s)}{br} \\ b(r-1) & s + \frac{1-s}{r} \end{bmatrix}. \tag{2.1.74}$$

The characteristic polynomial of (2.1.74) is

$$P(\lambda) = \lambda^2 - a\lambda + a_2 = \lambda^2 - (1 + s + \frac{1-s}{r})\lambda + 1. \tag{2.1.75}$$

We apply the Jury test and have

$$P(-1) = 1 + 1 + s + \frac{1-s}{r} + 1 > 0, \tag{2.1.76}$$

$$P(1) = 1 - 1 - s - \frac{1-s}{r} + 1 = (1-s)(1 - \frac{1}{r}) > 0, \tag{2.1.77}$$

$$a_2 = 1. \tag{2.1.78}$$

Lemma 2.1.7 *The eigenvalues of the Jacobian matrix (2.1.74) are complex conjugates of absolute value 1.*

Proof: The characteristic polynomial (2.1.75) is a concave-up parabolic. It has a minimum at $\lambda^* = \frac{(1+s+\frac{1-s}{r})}{2}$. Since $P(\lambda^*) > 0$ for $r > 1$, the equation $\lambda^2 - (1 + s + \frac{1-s}{r})\lambda + 1 = 0$ has complex roots $\lambda_1 = \bar{\lambda_2}$. Next, we know that

$$\lambda_1\bar{\lambda_2} = \frac{1}{4}\left(-a + \sqrt{a^2 - 4a_2}\right)\left(-a - \sqrt{a^2 - 4a_2}\right) = a_2. \tag{2.1.79}$$

Hence, the absolute value of eigenvalues is 1. ∎

Remark 2.1.8 Linear analysis does not determine the stability of coexistence equilibrium since $|\lambda| = 1$. However, numerical simulations indicate that the equilibrium is unstable as illustrated in Figure 2.15. Figure 2.12 shows one example that the system has a limit cycle.

In addition, at the coexistence equilibrium for $rf > 1$; i.e. $r > \frac{b}{1-s}$, we obtain

$$J(f^*, c^*) = \begin{bmatrix} 0 & \frac{-(1-s)^2}{b^2} \\ 0 & s + \frac{(1-s)^2}{b} \end{bmatrix}. \tag{2.1.80}$$

This coexistence equilibrium is stable if $s + \frac{(1-s)^2}{b} < 1$; or equivalently, $s + b > 1$.

If $r > 1$ and $s + b > 1$, both populations can coexist. Figure 2.12 shows a limit cycle occurs when $rf^* \leq 1$ ($r \leq \frac{b}{1-s}$). On the other hand, if we increase r such that $rf^* > 1$ ($r > \frac{b}{1-s}$), the solutions will reach a stable coexistence equilibrium as shown in Figure 2.13.

The consideration of consumer clumped search at aggregation degree one is able to stablize the model with Holling Type 1 growth function for the case $rf^* > 1$ only. In the case $rf^* < 1$, i.e. the inequality (2.1.71) is satisfied, our numerical simulation shows the system has oscillating resource and consumer densities. Figure 2.14, Figure 2.15, and Figure 2.16 show the consumer population at the last 35 generations of 10,000 generations with respect to different values of s, r, and b. Again, we observe that smaller r, larger s, or larger b leads to a bifurcation.

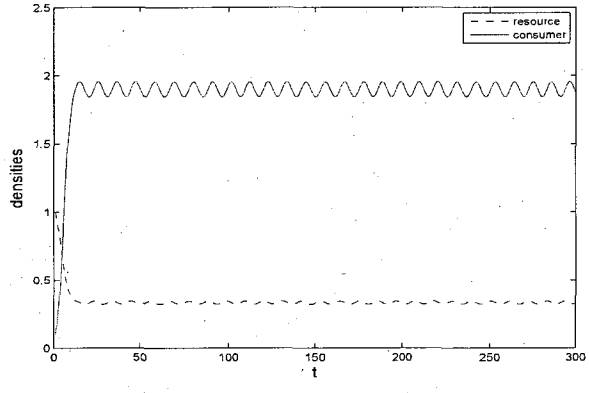

Figure 2.12: At $s = 0.5$, $b = 1.5$, $r = 2.9$, we have $rf^* \leq 1$ ($r \leq \frac{b}{1-s}$). Both resource and consumer densities have limit cycles.

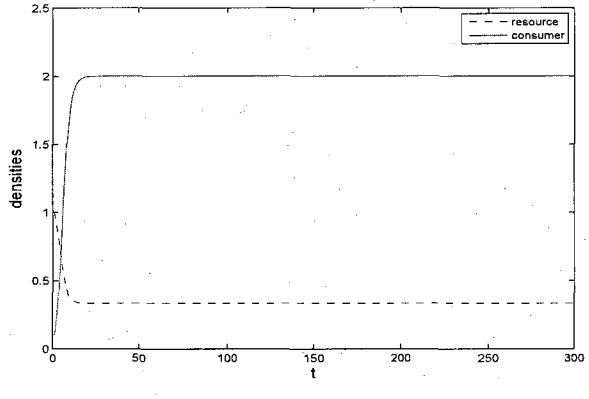

Figure 2.13: at $s = 0.5$, $b = 1.5$, $r = 3$, we have $rf^* > 1$ ($r > \frac{b}{1-s}$). Both resource and consumer densities converge to stable steady states.

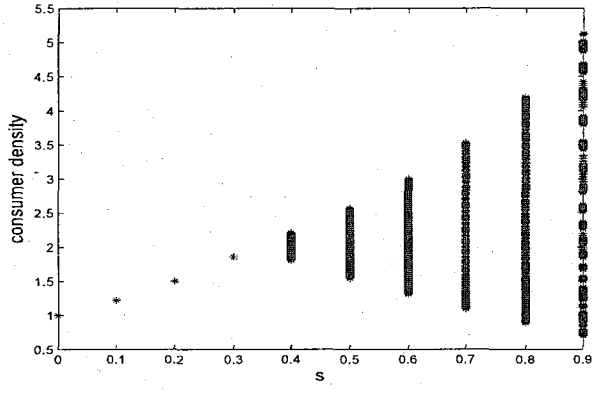

Figure 2.14: Bifurcation of model (2.1.63), (2.1.64), (2.1.65), (2.1.66) for increasing s with fixed $r = 3$, $b = 2$. A bifurcation is observed as s increases.

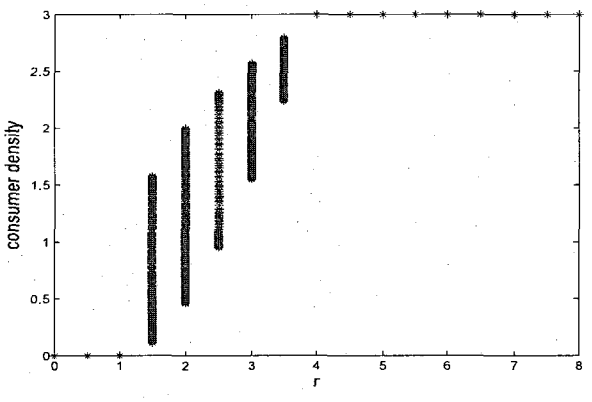

Figure 2.15: Bifurcation of model (2.1.63), (2.1.64), (2.1.65), (2.1.66) for increasing r with fixed $s = 0.5$, $b = 2$. A bifurcation is observed as r decreases.

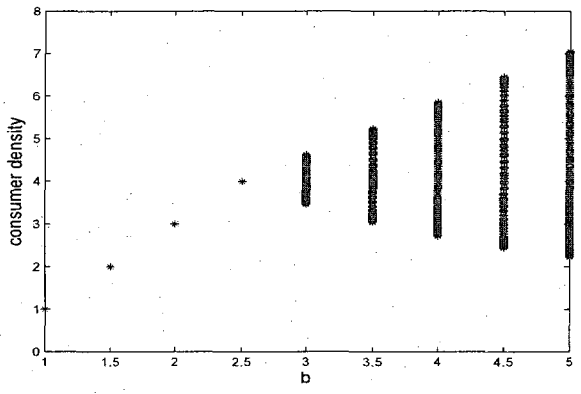

Figure 2.16: Bifurcation of model (2.1.63), (2.1.64), (2.1.65), (2.1.66) for increasing b with fixed $r = 5$, $s = 0.5$. A bifurcation is observed as b increases.

Neither resources nor consumers can persist if $r < 1$. If $r > 1$ but $s + b < 1$, only resources can persist and consumers go extinct. For $r > 1$ and $s + b > 1$, both populations can persist and the coexistence equilibrium is stable if the inequality (2.1.71) is not satisfied. Otherwise, there is a stable cycle for the coexsiting populations.

2.2 Overcompensatory Dynamics

We consider overcompensatory dynamics as described by the logistic growth function coupled with clumped search by consumers. Here, we denote $R = r - 1$. The resulting equations are:

$$F_{t+1} = \left[(1+R)F_t - \frac{R}{K}F_t^2\right]\frac{1}{1+\frac{aC_t}{L}} \tag{2.2.1}$$

$$C_{t+1} = sC_t + L\tilde{b}\left[(1+R)F_t - \frac{R}{K}F_t^2\right]\left(1 - \frac{1}{1+\frac{aC_t}{L}}\right). \tag{2.2.2}$$

We introduce the nondimensional quantities and rewrite (2.2.1) and (2.2.2) as

$$f_{t+1} = \left[(1+R)f_t - Rf_t^2\right]\frac{1}{1+c_t} \tag{2.2.3}$$

$$c_{t+1} = sc_t + b\left[(1+R)f_t - Rf_t^2\right]\left(1 - \frac{1}{1+c_t}\right). \tag{2.2.4}$$

If $f_t > \frac{1+R}{R}$ and $c_t = 0$, $f_{t+1} < 0$. Therefore, we need to find a reasonable range for R such that $f_{t+1} \geq 0$ for all t.

Lemma 2.2.1 *If* $0 < R \leq 3$, *then the domain* $\left[0, \frac{R+1}{R}\right]$ *is invariant for* $f_{t+1} = G(f_t)$.

Proof: Suppose $G(f) = (1+R)f - Rf^2$. We know that $G(f) = 0$ at $f = \frac{1+R}{R}$. We find that G has a maximum at $f = \frac{1+R}{2R}$. Next, we set $G(\frac{1+R}{2R}) \leq \frac{1+R}{R}$ for $G \geq 0$ and conclude that $R \leq 3$ to ensure $f > 0$ for all t. ∎

This model has three equilibria as well: the trivial equilibrium $(0,0)$, the semi-trivial equilibrium $(1,0)$, and coexistence equilibrium

$$f^* = \frac{1-s}{b},\ c^* = R\left(1 - \frac{1-s}{b}\right). \tag{2.2.5}$$

The coexistence equilibrium is biologically meaningful for $s + b > 1$.

The system of equations (2.2.3) and (2.2.4) yields the Jacobian matrix:

$$J(f,c) = \begin{bmatrix} \frac{1+R-2Rf}{1+c} & -\frac{(1+R)f - Rf^2}{(1+c)^2} \\ \frac{bc(1+R-2Rf)}{1+c} & s + \frac{b[(1+R)f - Rf^2]}{(1+c)^2} \end{bmatrix}. \tag{2.2.6}$$

At the trivial equilibrium, the Jacobian matrix is given by

$$J(0,0) = \begin{bmatrix} 1+R & 0 \\ 0 & s \end{bmatrix}. \tag{2.2.7}$$

The trivial equilibrium is always unstable as $1 + R > 1$ for a positive R. At the semi-trivial equilibrium, the Jacobian matrix is given by

$$J(1,0) = \begin{bmatrix} 1-R & -1 \\ 0 & s+b \end{bmatrix}. \tag{2.2.8}$$

The semi-trivial equilibrium is thus stable if $0 < R < 2$ and $s + b < 1$. In addition, at the coexistence equilibrium, the Jacobian matrix is given by

$$J(f^*, c^*) = \begin{bmatrix} \frac{b(1+R)-2R(1-s)}{b(1+R)-R(1-s)} & \frac{s-1}{b(1+R)-R(1-s)} \\ \frac{R(b-1+s)b[(1+R)-2R(1-s)]}{b(1+R)-R(1-s)} & s + \frac{b(1-s)}{b(1+R)-R(1-s)} \end{bmatrix}. \tag{2.2.9}$$

Lemma 2.2.2 *The coexistence steady state is stable if*

$$b > \frac{R(5 - 4s - s^2)}{4 + 3R + Rs}. \tag{2.2.10}$$

Proof: The characteristic polynomial from the Jacobian matrix (2.2.9) is

$$\begin{aligned} P(\lambda) &= \lambda^2 - a_1\lambda + a_2 \\ &= \lambda^2 + \left[-1 - s - \frac{(1-s)(b-R)}{b(1+R) - R(1-s)}\right]\lambda + \left(1 - \frac{R(1-s)}{b(1+R) - R(1-s)}\right). \end{aligned}$$

We apply the Jury test and obtain the following three ineqalities

$$P(-1) = 1 + 1 + s + \frac{(1-s)(b-R)}{b(1+R) - R(1-s)} + 1 - \frac{R(1-s)}{b(1+R) - R(1-s)} > 0, \tag{2.2.11}$$

$$P(1) = 1 - 1 - s - \frac{(1-s)(b-R)}{b(1+R) - R(1-s)} + 1 - \frac{R(1-s)}{b(1+R) - R(1-s)} > 0, \tag{2.2.12}$$

$$a_2 = 1 - \frac{R(1-s)}{b(1+R) - R(1-s)} < 1. \tag{2.2.13}$$

The inequalities (2.2.11), (2.2.12), and (2.2.13) can be further reduced to

$$\begin{aligned} P(-1) &= 3 + s + \frac{(1-s)(b-2R)}{b(1+R) - R(1-s)} \\ &= \frac{b(4 + 3R + Rs) - 5R + 4Rs + Rs^2}{b(1+R) - R(1-s)} > 0, \end{aligned} \tag{2.2.14}$$

$$P(1) = 1 - s - \frac{(1-s)(b-2R)}{b(1+R) - R(1-s)}$$

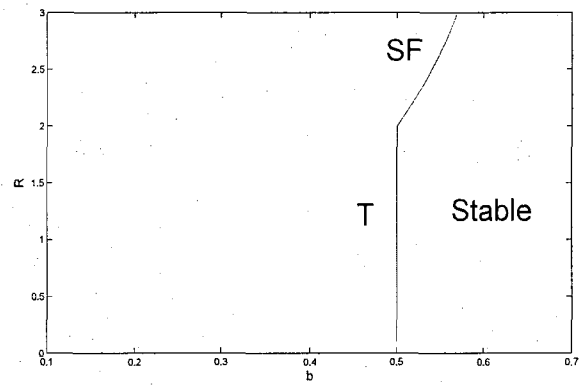

Figure 2.17: Region of stability for the model (2.2.3), (2.2.4) for s=0.5. Boundary T corresponds to a transcritical bifurcation. Boundary SF corresponds to a subcritical flip bifurcation.

$$= \frac{(1-s)(bR+R+Rs)}{b(1+R)-R(1-s)} > 0, \tag{2.2.15}$$

$$a_2 = \frac{b(1+R)-2R(1-s)}{b(1+R)-R(1-s)} < 1. \tag{2.2.16}$$

Since $s+b>1$, $b(1+R)-R(1-s) = b+R(b+s-1) > 0$. Thus, inequalities (2.2.15) and (2.2.16) are always satisfied. In addition, the inequality (2.2.14) is satisfied if

$$R > \frac{-4b}{s^2+(b+4)s+3b-5}.$$

Hence, the coexistence equilibrium is stable if the inequality (2.2.10) is satisfied. ∎

Figure 2.17 shows the stable region of the model (2.2.3), (2.2.4) which is bounded by the curves of $b > \frac{R(5-4s-s^2)}{4+3R+Rs}$ and $s+b=1$ for $s=0.5$.

For $R<2$, the consumer can persist in the system where $s+b>1$. For $R>2$, however, $s+b>1$ is not sufficient for consumer persistence, see Figure 2.18. For fixed $s+b>1$, there is a flip bifurcation as we increase R so that (2.2.14) is violated.

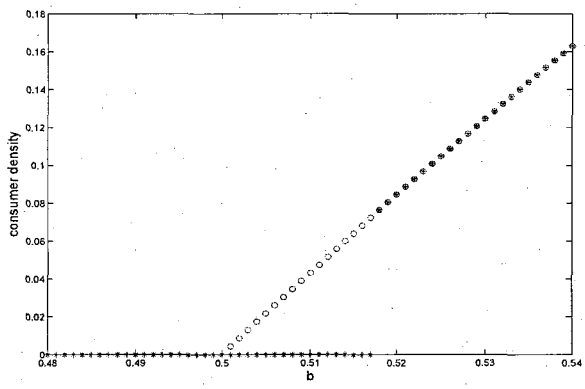

Figure 2.18: Consumer population at the steady state for model (2.2.3), (2.2.4) (*) and for the formula (2.2.5) (o) for increasing b with fixed $s = 0.5$, $R = 2.2$.

That is, when R is increasing, an eigenvalue is passing through $\lambda = -1$ and we would expect a stable two-cycle of both populations. However, the numerical simulation reveals that the consumer is lost from the system and the resource persists in a stable two-cycle provided $R > 2$ is small enough. A similar behavior was observed by Neubert and Kot [24] in a slightly different discrete-time consumer-resource model. Hence, the coexistence steady state loses its stability in a subcritical flip bifurcation [16].

If we replace the clumped search in (2.2.1), (2.2.2) by random search, we expect that the behavior is similar, except that large values of b might lead to a Neimark-Sacker bifurcation. The steady state is given implicitly by

$$f^* = 1 + \frac{e^{c^*} - 1}{R}, c^* = \frac{b}{1-s} f^* \left(e^{c^*} - 1\right). \tag{2.2.17}$$

Numerical simulations confirm that consumers have oscillating populations for large values of b. (Figure 2.20 shows one example).

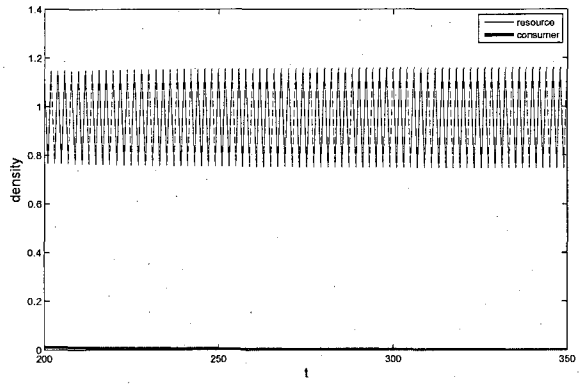

Figure 2.19: At $b = 0.51$, $s = 0.5$, $R = 2.2$, the consumer cannot invade the system. The resource density has a stable 2-cycle.

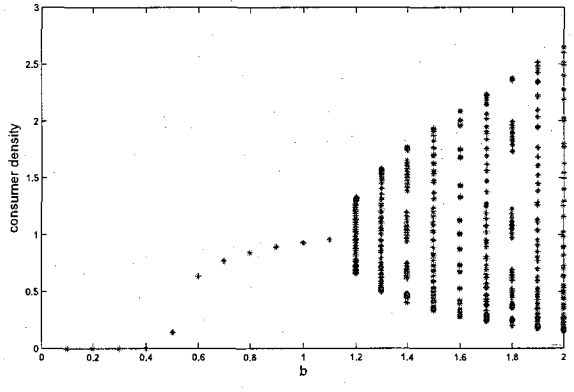

Figure 2.20: Consumer population at the steady state for model (2.2.3), (2.2.4) with the random search function for increasing b with fixed $s = 0.5$, $R = 2.2$.

2.3 Summary

In this chapter, we considered the non-spatial consumer-resource models for various different growth and consumption functions. Each model has the trivial and semi-trivial equilibrium. If $r < 1$ for the compensatory dynamics or $R < 0$ for the overcompensatory dynamics, the trivial equilibrium is stable. The extinction of resource results in the extinction of consumer. Next, if $r > 1$ for the compensatory dynamics or $R > 0$ for the overcompensatory dynamics, and $s + b < 1$, the semi-trivial equilibrium is stable. Although the resource can survive with $r > 1$ or $R > 0$, the consumer cannot persist due to too small survival rate or too small conversion coefficient.

If $r > 0$ and $s + b > 1$, both populations can persist. Their populations could reach a stable equilibria under certain conditions. For example, the coexistence equilibrium in the model with Beverton-Holt and negative exponential functions is stable if $\frac{se^c}{r} + \frac{be^{2c}(re^{-c}-1)}{r(r-1)} < 1$. If we consider the clumped search by consumers; i.e. we apply the negative binomial function for the probability of resource being consumed successfully, the coexistence equilibrium might become stable for all parameters. For instance, the coexistence equilibrium in the model with Beverton-Holt growth function is always stable.

The coexsitence equilibrium in the model with Holling Type 1 growth function has two cases: $rf^* \leq 1$ and $rf^* > 1$. For the case $rf^* > 1$, the coexistence equilibrium is stable for the random search by consumer if $\frac{b}{1-s} - c^* < 1$ and always stable for the clumped search by consumer. For the case $rf^* \leq 1$, the coexistence equilibrium is always unstable for both random search and clumped search by consumer.

There is also a condition ($b > \frac{R(5-4s-s^2)}{4+3R+Rs}$) for the coexistence equilibrium in the model with Logistic and negative exponential functions to be stable. However, there is also a restriction $R < 3$. Too large R causes the resource to increase significantly, but it also causes the resource population to reduce to zero in the next generation

because of the characteristic of overcompensatory growth dynamics.

In our models with compensatory growth dynamics, a smaller value of s or b as well as a larger value of r leads the system to converge to a stable steady state. The case of clumped seach by consumers stablizes the system. For the model with the logistic (overcompensatory) growth dynamics and the negative binomial function, consumers cannot persist in the system for $s + b < 1$. A larger value of R can result in a two-cycle for the resource and extinction for the consumer. If the negative exponential function is applied instead of the negative binomial function, we observe a Neimark-Sacker bifurcation as we increase b.

Chapter 3

Spatial Dynamics

Consumers generally do not disperse evenly over the resource patch in the search of food because moving farther from the central place to forage requires more energy. Therefore, most consumers distribute over the habitat which is close to the central place. The foraging distribution is no longer a uniform kernel and the resource-consumer model becomes spatial. In this chapter, we choose the Beverton Holt growth function for G to eliminate overcompensatory density dependence in order to focus on the dynamics of space generated by spatial redistribution only. We focus on the stability of the coexistence equilibrium. We assume that while the spatial distribution of consumers is not homogeneous, this distribution is constant in time. In addition, we consider that consumers position themselves symmetrically around the central location and their density decrease exponentially as their foraging location from the central place increases. Hence, we apply the Laplace kernel

$$k(x) = \frac{\alpha_L e^{-\alpha_L |x|}}{2} \tag{3.0.1}$$

to represent the distribution of consumers, where a larger value of α_L gives a smaller value of variance $\frac{2}{\alpha_L^2}$. We assume more than 98 percent of consumers foraging in the foraging domain of length $L = 1$ (Consumers outside the foraging domain do not

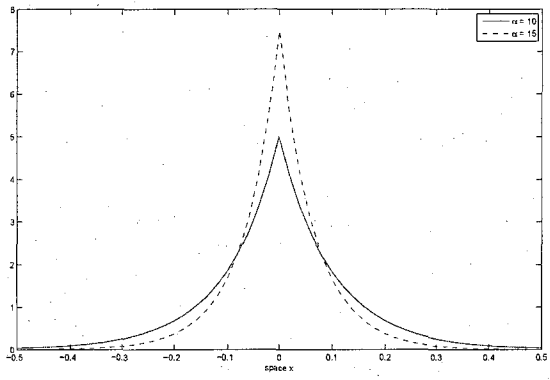

Figure 3.1: The Laplace kernel has a back-to-back exponential curve whose slope is steeper as α_L increases.

acquire any food) by setting $\alpha_L \geq 10$ so that $\int_{-L}^{L} k(x)dx > 0.98$. The Laplace kernel can be derived from a system of PDEs which we will discuss in the next chapter. Figure 3.1 shows two Laplace kernels with different variances.

In this chapter, we do not consider energy discount in the model with a fixed kernel in order to compare the dynamics between spatial and non-spatial model. We will study the energy discount function in the model with the resource-dependent kernel in Chapter 5.

3.1 Negative Exponential Probability

First, we apply the negative exponential probability function to describe consumer foraging success. We obtain the following spatial consumer-resource model

$$F_{t+1}(x) = \frac{rF_t(x)}{1+\frac{r-1}{K}F_t(x)} \exp\left(-a_F C_t k(x)\right), \tag{3.1.1}$$

$$C_{t+1} = sC_t + \tilde{b}\int_{-L/2}^{L/2} \frac{rF_t(x)}{1+\frac{r-1}{K}F_t(x)} \left[1-\exp\left(-a_F C_t k(x)\right)\right] dx. \tag{3.1.2}$$

We introduce the same nondimensional quantities used in the Chapter 2 and scale $L\tilde{x}$ as x, $\tilde{k}(\tilde{x})$ as $k(x)$ where the variance becomes $\frac{2}{\tilde{\alpha}^2} = \frac{2}{\alpha_L^2 L^2}$. For the sake of notation, we write $\tilde{x}$ as x; $\tilde{k}$ as k; $\tilde{\alpha_L}$ as α_L. Equations (3.1.1), (3.1.2) thus change to

$$f_{t+1}(x) = \frac{r f_t(x)}{1 + (r-1) f_t(x)} \exp\left(-c_t k(x)\right), \tag{3.1.3}$$

$$c_{t+1} = s c_t + b \int_{-1/2}^{1/2} \frac{r f_t(x)}{1 + (r-1) f_t(x)} \left[1 - \exp\left(-c_t k(x)\right)\right] dx. \tag{3.1.4}$$

The coexistence steady state of this system is not spatially homogeneous. The steady state formula for the resource is

$$f^*(x) = \frac{r f^*(x)}{1 + (r-1) f^*(x)} \exp\left(-c^* k(x)\right). \tag{3.1.5}$$

Since $f^*(x)$ may be zero for some x (for example, the resources could be completely depleted near the central place), we cannot simply cancel $f^*(x)$ from the equation (3.1.5). Suppose $f^*(x) \neq 0$, then $f^*(x)$ is given by

$$f^*(x) = \frac{r \exp\left(-c^* k(x)\right) - 1}{r - 1}. \tag{3.1.6}$$

Since $f^*(x) \geq 0$ for all x, we have $f^*(x) = 0$ if $r \exp(-c^* k(x)) < 1$. Since $k(x)$ is monotonically decreasing for positive x, the expression $r \exp(-c^* k(x)) - 1$ is monotocially increasing for positive x. Hence, there is some $m \geq 0$ such that

$$f^*(x) = \begin{cases} 0, & |x| \leq m, \\ \frac{r \exp(-c^* k(x)) - 1}{r-1}, & m < |x| \leq \frac{L}{2}, \end{cases} \tag{3.1.7}$$

$$\begin{aligned} c^* &= \frac{b}{1-s} \int_{-1/2}^{1/2} f^*(x) \left[\exp(c^* k(x)) - 1\right] dx \\ &= \frac{2b}{(1-s)(r-1)} \int_m^{1/2} \left[-r \exp(-c^* k(x)) - \exp(c^* k(x)) + r + 1\right] dx. \end{aligned} \tag{3.1.8}$$

For the Laplace kernel, we can implicitly calculate

$$m = \frac{\ln(c^* \alpha_L) - \ln(2 \ln(r))}{\alpha_L}. \tag{3.1.9}$$

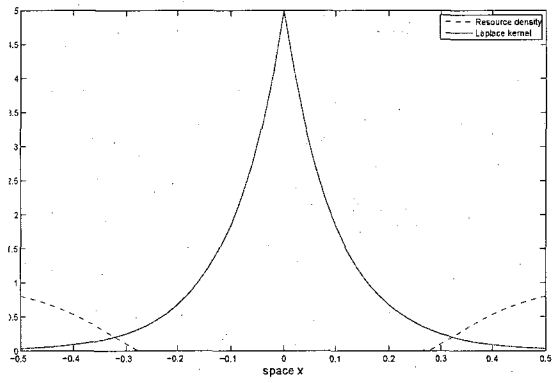

Figure 3.2: Steady state resource distribution (dashed) and foraging kernel (solid) at $b = 20$, $r = 5$, $s = 0.5$, $\alpha_L = 10$. $f(x) = 0$ for $|x| < 0.26$.

This expression then can be used in (3.1.8) to numerically obtain c^*. Similar to models with the uniform kernel, the parameters s, r, and b affect the stability of the coexistence equilibrium. In addition, the shape of the Laplace kernel influences the stability as well. However, since we cannot explicitly determine the steady state solution, we revert to numerical simulation of the system to determine stability of the coexistence steady state.

The effect of α_L

The resource population is low at the place where more consumers forage. Increase of α_L means increasing number of consumers foraging near the central location. From the formula (3.1.9), we expect that m decreases as α_L increases. By comparing Figure 3.2 and Figure 3.3, we observe that the area, where the resource population is zero, is larger for smaller values of α_L.

From Figure 3.4, we know that the increase of α_L stablizes the system. Although consumers foraging near the central place will not find any resource there, the places at the two ends of the foraging domain provide sufficient resources for the entire consumer population to survive. Figure 3.4 shows that the consumer population

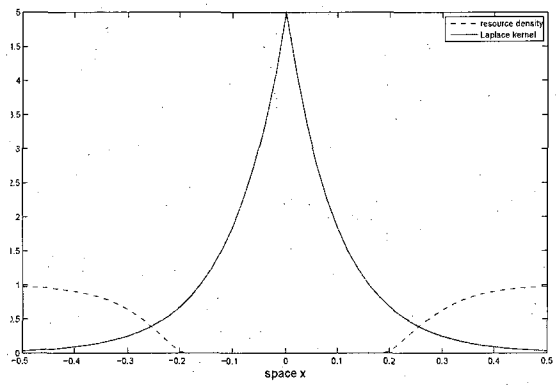

Figure 3.3: Steady state resource distribution (dashed) and foraging kernel (solid) at $b = 20$, $r = 5$, $s = 0.5$, $\alpha_L = 11$. $f(x) = 0$ for $|x| < 0.18$

converges to a stable equilibrium as α_L increases.

The effect of r, b, and s

The parameters r and b in this spatial model have the same effects as the ones in the non-spatial model on the stability of coexistence equilibrium: decreasing r or increasing b leads the consumer density to a bifurcation as shown in Figure 3.5 and Figure 3.6. We denote this kind of bifurcation as the Neimark-Sacker bifurcation in this thesis since an invariant loop is observed. However, we are aware that the types of bifurcation are hard to be determined since we cannot find eigenvalues implicitely and the model has infinite dimensions.

On the other hand, the stability properties of the coexistence steady state with respect to the parameter s in the spatial model are opposite to those of the non-spatial model.

The higher consumer survival rate s in the model (3.1.3), (3.1.4) leads to instability of the coexistence equilibrium and a Neimark-Sacker bifurcation occurs as illustrated in Figure 3.7.

Figure 3.8 indicates the stable region with respect to r and b at $s = 0.5$ for

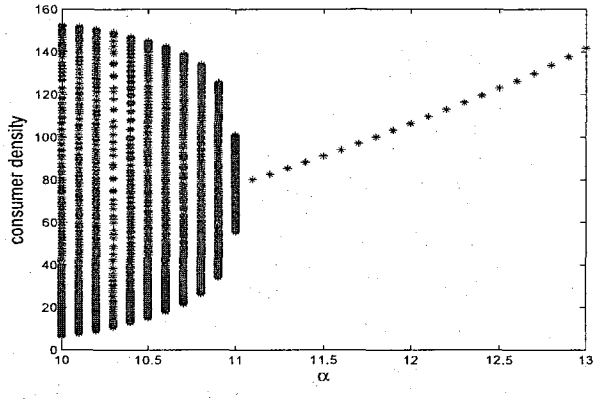

Figure 3.4: Bifurcation of model (3.1.3), (3.1.4) for increasing α_L with fixed $r = 11$, $s = 0.5$, $b = 2000$. A Neimark-Sacker bifurcation is observed as α_L decreases.

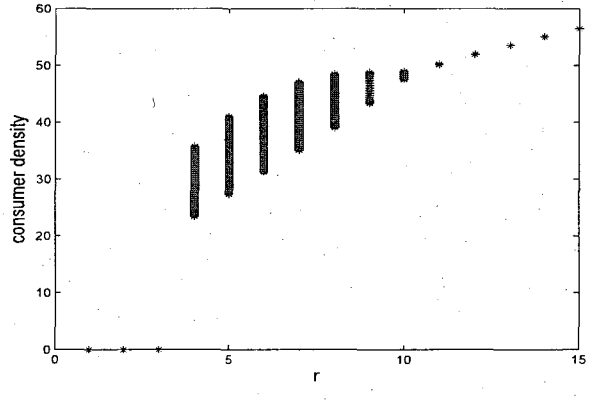

Figure 3.5: Bifurcation of model (3.1.3), (3.1.4) for increasing r with fixed $\alpha_L = 10$, $s = 0.5$, $b = 1030$. A Neimark-Sacker bifurcation is observed as r decreases.

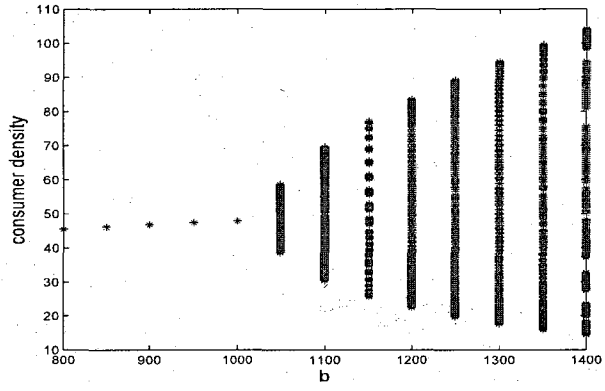

Figure 3.6: Bifurcation of model (3.1.3), (3.1.4) for increasing b with fixed $r = 10$, $s = 0.5$, $\alpha_L = 10$. A Neimark-Sacker bifurcation is observed as b increases.

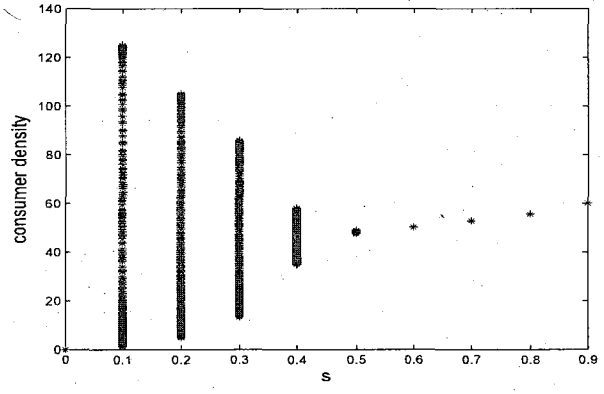

Figure 3.7: Bifurcation of model (3.1.3), (3.1.4) for increasing s with fixed $r = 10$, $\alpha_L = 10$, $b = 1030$. A Neimark-Sacker bifurcation is observed as s decreases.

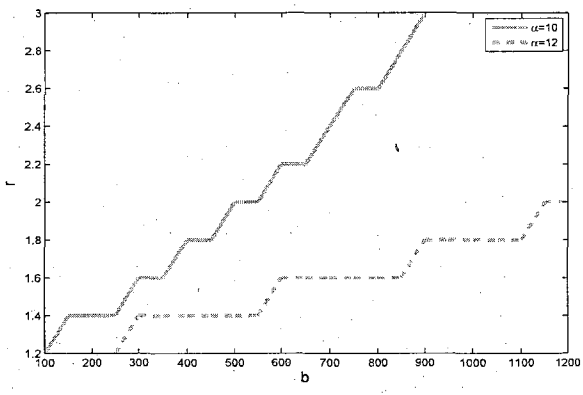

Figure 3.8: Stable and unstable region of model (3.1.3), (3.1.4) at $s = 0.5$, $\alpha_L = 10, 12$

$\alpha_L = 10$ and $\alpha_L = 12$. The values of r and b located at the left side of the curve lead the consumer density to a limit cycle.

3.2 Negative Binomial Probability

As can be seen in the non-spatial model, the solution of consumer-resource system could converge to a stable coexistence equilibrium if the consumer clumps to search for the resource. In this section, we apply the negative binomial probability function to determine the effect of aggregation of consumers upon the stability of coexistence equilibrium in the spatial model. By applying the Laplace kernel, we obtain

$$F_{t+1}(x) = \frac{rF_t(x)}{1+\frac{r-1}{K}F_t(x)} \frac{1}{1+a_F C_t \frac{\alpha_L \exp(-\alpha_L|x|)}{2}} \tag{3.2.1}$$

$$C_{t+1} = sC_t + \tilde{b}\int_{-L/2}^{L/2} \frac{rF_t(x)}{1+\frac{r-1}{K}F_t(x)} \left[1 - \frac{1}{1+a_F C_t \frac{\alpha_L \exp(-\alpha_L|x|)}{2}}\right] dx. \tag{3.2.2}$$

We nondimensionalize equations (3.2.1), (3.2.2) with the same nondimensional quantities and notations introduced in the previous section, and this spatial model changes

to

$$f_{t+1}(x) = \frac{rf_t(x)}{1+(r-1)f_t(x)} \frac{1}{1+c_t\frac{\alpha_L \exp(-\alpha_L|x|)}{2}}, \tag{3.2.3}$$

$$c_{t+1} = sc_t + b\int_{-1/2}^{1/2} \frac{rf_t(x)}{1+(r-1)f_t(x)} \left[1 - \frac{1}{1+c_t\frac{\alpha_L \exp(-\alpha_L|x|)}{2}}\right] dx. \tag{3.2.4}$$

This system has the coexsitence steady state

$$f^*(x) = \begin{cases} 0, & |x| \le m, \\ \frac{\frac{r}{1+c^*k(x)}-1}{r-1}, & m < |x| \le \frac{1}{2}, \end{cases} \tag{3.2.5}$$

$$\begin{aligned} c^* &= \frac{b}{1-s}\int_{-1/2}^{1/2} f^*(x)\frac{c^*k(x)}{1+c^*k(x)}dx \\ &= \frac{2b}{(1-s)(r-1)}\int_m^{1/2} \left(\frac{r}{1+c^*k(x)} - 1\right)\left(\frac{c^*k(x)}{1+c^*k(x)}\right) dx. \end{aligned} \tag{3.2.6}$$

The expression (3.2.5) is monotonically increasing for $m < x < 1/2$. We solve $f^*(x) = 0$ to obtain

$$m = \frac{\ln(c^*\alpha_L/2(r-1))}{\alpha_L}. \tag{3.2.7}$$

Similar to the previous section, the resource near the central place is depleted as well as the depleted area is smaller with larger α_L as illustrated in Figure 3.9 and Figure 3.10.

However, by comparing Figure 3.2 and Figure 3.3 to Figure 3.9 and Figure 3.10, we find that the domain where the resource is completely diminished are smaller for the model with clumped search by the consumer.

In contrast to the model with random search by the consumer, our numerical simulations indicate that the coexistence equilibrium in this spatial model is stable for some given ranges of parameters. Figure 3.11, Figure 3.12, Figure 3.13, and Figure 3.14 are examples showing the consumer density converges to a stable steady state with respect to s, r, b, and α_L respectively. By comparing this model to other

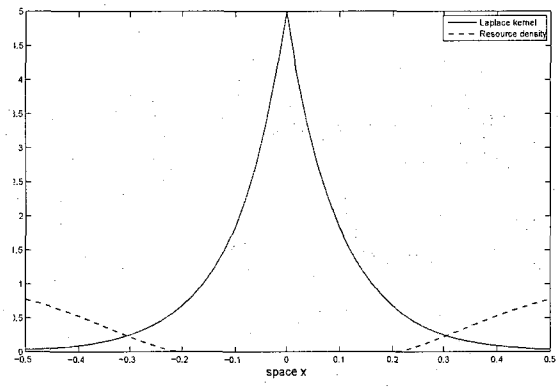

Figure 3.9: Steady state resource distribution (dashed) and foraging kernel (solid) at $b = 20$, $r = 5$, $s = 0.5$, $\alpha_L = 10$. $f(x) = 0$ for $|x| < 0.2$

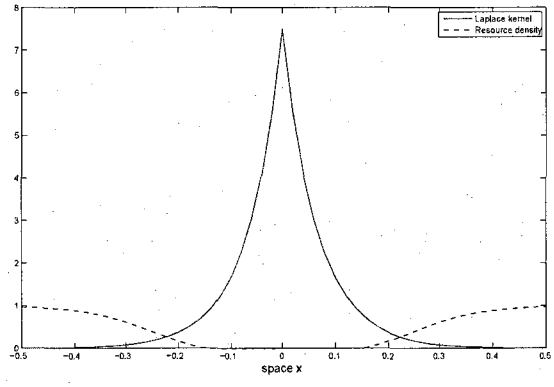

Figure 3.10: Steady state resource distribution (dashed) and foraging kernel (solid) at $b = 20$, $r = 5$, $s = 0.5$, $\alpha_L = 15$. $f(x) = 0$ for $|x| < 0.14$

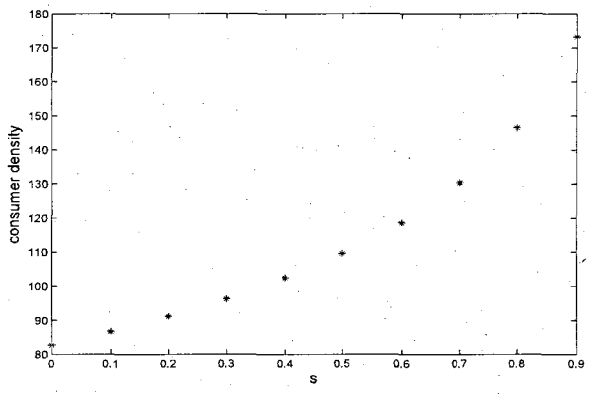

Figure 3.11: Consumer densities of model (3.2.3), (3.2.4) for increasing s with fixed $r = 10$, $\alpha_L = 10$, $b = 1000$. The consumer density converges to a stable steady state for all s

non-spatial models with negative binomial functions, we expect the solutions of this system converge to stable steady states.

3.3 Summary

The Laplace foraging kernel represents the phenomenon that consumers tend to stay close to the central place to forage. It results in the depletion of resources near the central location. We explored this scenario numerically. If the resource is consumed successfully according to the negative binomial function, the system will reach a stable coexistence equilibrium. If the probability of resource being consumed successfuly is described by the negative exponential function, the coexistence equilibrium is only stable for larger values of s, r, α_L, or smaller values of b.

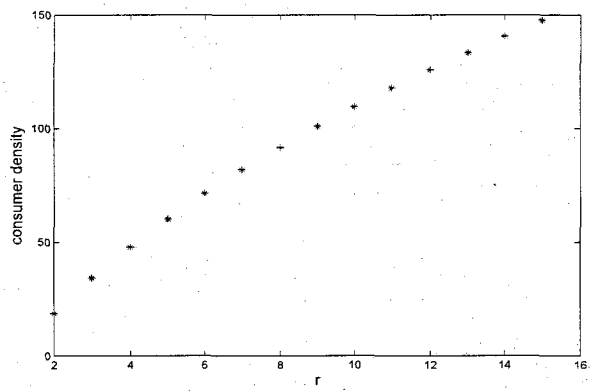

Figure 3.12: Consumer densities of model (3.2.3), (3.2.4) for increasing r with fixed $s = 0.5$, $\alpha_L = 10$, $b = 1000$. The consumer density converges to a stable steady state for all r

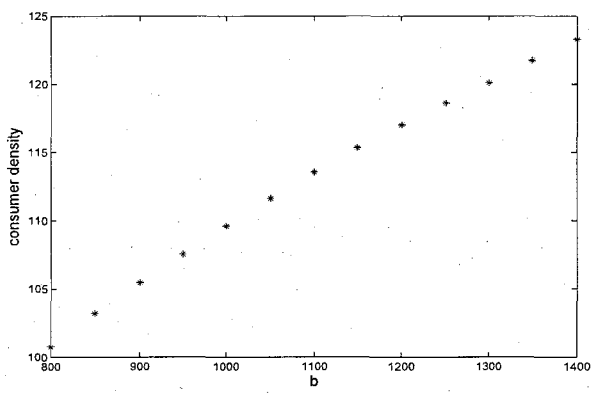

Figure 3.13: Consumer densities of model (3.2.3), (3.2.4) for increasing b with fixed $r = 10$, $\alpha_L = 10$, $s = 0.5$. The consumer density converges to a stable steady state for all b

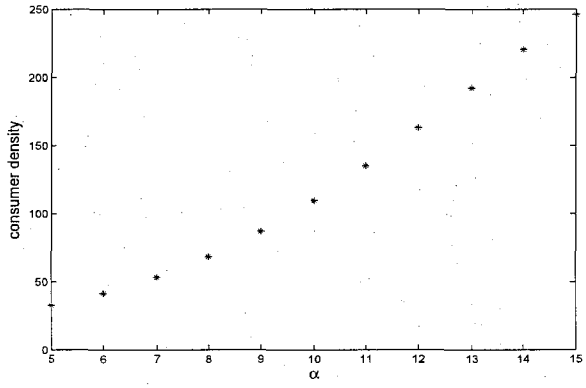

Figure 3.14: Consumer densities of model (3.2.3), (3.2.4) for increasing α_L with fixed $r = 10$, $s = 0.5$, $b = 1000$. The consumer density converges to a stable steady state for all α_L

Chapter 4

Resource-Dependent Foraging Kernel

In the previous chapter, we noticed that the resource near the central place is typically depleted due to the aggregation of consumers at the central place. However, assuming a fixed kernel implies that consumers still forage at the location with low resources. Fagan et al [9] introduced a maximization scheme to account for "adaptive" foraging. They fixed the functional form of a chosen kernel and varied parameters every time step as to optimize population-level food intake. This approach assumes that consumers can communicate with one another. In addition, it prescribes the functional form of foraging kernel. Here, we use an approach based on the individual movement behavior to find foraging locations. In this chapter, we assume that the resource density is fixed in order to explain our approach. We discuss the population dynamical implications in the next chapter.

We consider the following scenario. Consumers emerge from the central place, move randomly across the landscape, and settle at some location to forage. Then consumers return back to the central place in a fast and direct way. Consumers do not forage while they are moving. Once consumers settle, they stay there until

they return back to the central place. Alternatively, we assume that consumers make several foraging trips per season, but return to the same foraging location in every trip. For example, most penguins return repeatedly to the same area to forage [3]. We also assume that the time consumers spend to reach the foraging location is short compared to the foraging season.

4.1 Random Movement, Resource-Independent Settling

Many animals appear to disperse according to a reaction diffusion model with a constant diffusion coefficient [15] [21]. We apply the classical diffusion equation

$$u_t = Du_{xx}, \tag{4.1.1}$$

where D is a constant, with the initial condition $u(0,x) = \delta(x)$ to describe the probability density function for an individual's location at time t, $u(x,t)$. The solution to this initial value problem is

$$u(x,t) = \frac{e^{-x^2/4Dt}}{2\sqrt{\pi Dt}}, \tag{4.1.2}$$

which is the probability density function for the normal distribution.

Next, we consider that each individual settles at rate a. Then the PDEs representing the densities of moving (u) and settled (v) individuals are

$$u_t = Du_{xx} - au, \tag{4.1.3}$$

$$v_t = au \tag{4.1.4}$$

with the initial conditions $u(0,x) = \delta(x)$ and $v(0,x) = 0$. The distribution of consumers is given by $k(x) = \lim_{t\to\infty} v(t,x)$ provided that the foraging season is long enough for all individuals to settle.

Lemma 4.1.1 *[25] The coupled equations (4.1.3) and (4.1.4) result in the foraging kernel*

$$k(x) = \frac{\sqrt{\frac{a}{D}}}{2} \exp(-\sqrt{\frac{a}{D}}|x|). \tag{4.1.5}$$

Proof: We integrate the equation (4.1.3) from $t = 0$ to $t = \infty$ to yield

$$u(x,\infty) - u(x,0) = D\frac{\partial^2}{\partial x^2}\left[\frac{v(x,\infty)}{a} - \frac{v(x,0)}{a}\right] - v(x,\infty). \tag{4.1.6}$$

At $t = \infty$, there is no moving individual. Thus, from (4.1.6), we have

$$-\delta(x) = \frac{D}{a}\frac{\partial^2 k(x)}{\partial x^2} - k(x). \tag{4.1.7}$$

Next, we solve $\frac{D}{a}\frac{\partial^2 k(x)}{\partial x^2} - k(x) = 0$ for $x > 0$ and obtain the solution $k(x) = Ae^{-\sqrt{\frac{a}{D}}x}$ for some A. We note that $k(x) \to 0$ as $x \to \infty$. Similarly, we have another solution $k(x) = Be^{\sqrt{\frac{a}{D}}x}$ for some B for $x < 0$. Since $k(x)$ is continuous at $x = 0$, we have $A = B$. Then we can find $A = \frac{\sqrt{\frac{a}{D}}}{2}$ by solving $\int k(x)dx = 1$. Hence, the foraging kernel derived from equations (4.1.3) and (4.1.4) is given by

$$k(x) = \frac{\sqrt{\frac{a}{D}}}{2} \exp(-\sqrt{\frac{a}{D}}|x|)$$

∎

The distribution of a consumer who has a constant settling rate is the Laplace kernel. We have studied the population dynamic consequences of this foraging kernel in Chapter 3.

4.2 Random Movement, Resource-Dependent Settling

More realisitically, an individual's decision on whether to settle and forage is based on the availability of resource at a location. Therefore, we propose the situation that the

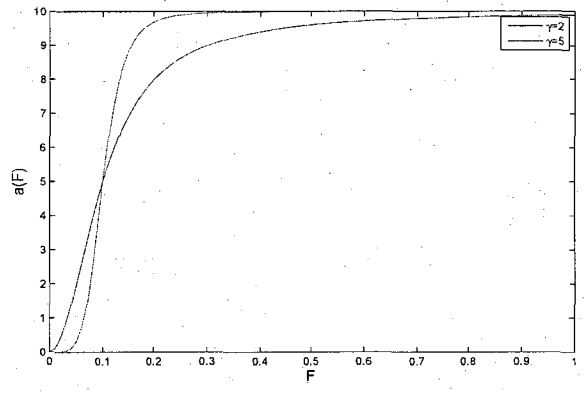

Figure 4.1: Hill equations at $\gamma = 2$ and $\gamma = 5$ with fixed $\alpha = 10$ and $\beta = 0.1$.

settling rate depends on the resource $F(x)$. The settling rate function $a(F)$ should be non-decreasing. The Hill function was originally derived by Archibold Hill in 1913 to show the sigmoidal shape of the oxygen dissociation curve (Chapter 4 in [8]). We apply the Hill's equation to describe the resource-dependent settling rate

$$a(F) = \alpha \frac{F^\gamma}{\beta^\gamma + F^\gamma}. \tag{4.2.1}$$

where α is the maximum settling rate; β is the half-saturation constant since $a(\beta) = \frac{\alpha}{2}$. γ is related to the maximum slope of $a(F)$.

The settling rate increases up to α as the resource density increases. An increase of α or decrease of β causes the settling rate to reach its upper bound faster. From Figure 4.1, we note that the Hill function equation with a higher value of γ has a steeper slope before it reaches to its maximum.

If β reduces to zero, the settling rate reaches the value of α immediately and the settling rate becomes a constant. The resulting distribution is the Laplace kernel $k(x) = \frac{\sqrt{\frac{a}{D}}}{2} \exp(-\sqrt{\frac{a}{D}}|x|)$. Similarly, if γ reduces to zero, the settling rate becomes a constant and the distribution of consumers is the Laplace kernel $k(x) = \frac{\sqrt{\frac{a}{2D}}}{2} \exp(-\sqrt{\frac{a}{2D}}|x|)$.

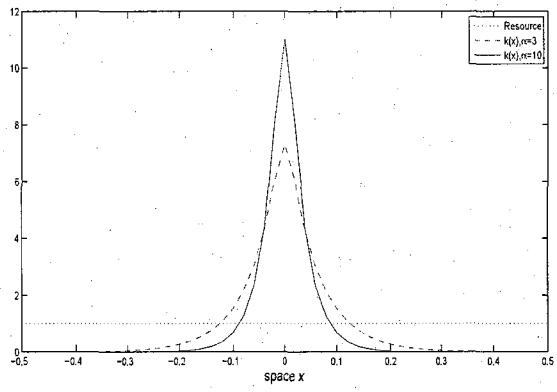

Figure 4.2: Resource-dependent foraging kernels at $\alpha = 3$ and $\alpha = 10$ with fixed $\beta = 0.1$, $\gamma = 2$ for the uniform resource distribution. These kernels are the Laplace kernels.

We use finite (forward) difference method to solve equations (4.1.3) and (4.1.4) to obtain the distribution of consumers. See Appendix for the Matlab codes for the numerical simulation of consumer-resource model with resource-dependent foraging kernel. We illustrate the effect of these parameters on the resulting foraging kernel for a fixed resource density. Figure 4.2 shows the case when the resource is homogeneous. Since the resource density is constant for all space x, the abundance of resource does not affect the consumer's decision on where to settle. Therefore, the settling rate is a constant and the resulting distribution is the Laplace kernal.

If resources near the central place are completely depleted, consumers do not settle at the location where there is no resource even though that location is close to the central place. Instead, they move farther to a location with sufficiently abundant resource to forage. For a non-constant resource profile, we choose

$$F(x) = \begin{cases} 0, & |x| \leq 0.1, \\ [2.5(|x| - 0.1)]^2, & |x| > 0.1. \end{cases} \tag{4.2.2}$$

We can expect that the resulting foraging kernel has two symmetric humps on both

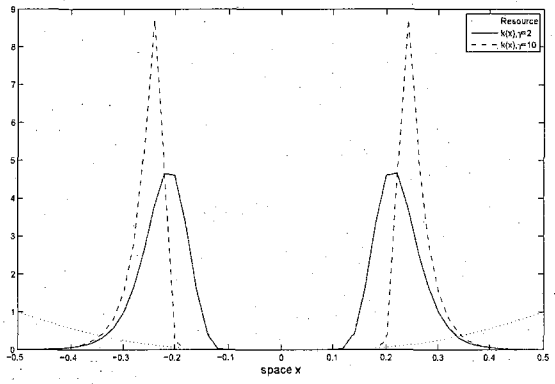

Figure 4.3: The resource-dependent foraging kernels at $\gamma = 2$ (solid) and $\gamma = 10$ (dashed) with fixed $\alpha = 10$, $\beta = 0.1$ for the non-homogeneous resource distribution (4.2.2). Both kernels have two humps symmetrically placed on both sides.

sides of central place as there is no consumer foraging at the centre. Figure 4.3, Figure 4.4, and Figure 4.5 show 2-peaks foraging kernels with different values of parameters.

A consumer might face the dilemma of settling at the place with higher resource density or with shorter distance from the central place. The decision can be interpreted by the parameters in the Hill equation. For instance, at $\alpha = 10$, $\beta = 0.1$, $\gamma = 2$, the mean distance that consumers travel from the central place is 0.2262 with variance 0.0022. According to Figure 4.3, we observe that if the consumer is more sensitive to the resource, i.e. γ is increased to 10, it will not settle at the place with very low resource. It is willing to move farther and thus the two humps of foraging kernel are farther from the centre. In this case, the mean distance increases to 0.2554 with the variance 0.0012.

Figure 4.4 and Figure 4.5 also demonstrate various two-peaked kernels by varing α and β respectively. With the original values of parameters we used in the previous paragraph ($\alpha = 10$, $\beta = 0.1$, $\gamma = 2$), we find the following. If we increase the value

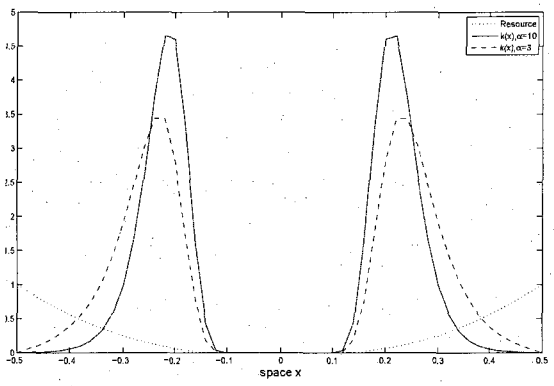

Figure 4.4: The resource-dependent foraging kernels at $\alpha = 3$ (dashed) and $\alpha = 10$ (solid) with fixed $\beta = 0.1$, $\gamma = 2$ for the non-homogeneous resource distribution (4.2.2). Both kernels have two humps symmetrically placed on both sides.

of β to 1, we expect the settling rate to decrease and the mean travelling distance to increase to 0.3111 with variance 0.0146. Similarly, if we reduce the value of α to 3, we expect the settling rate to decrease and the mean traveling distance to increase to 0.2549 with variance 0.005.

Next, we consider the situation that the resource is low but not completely depleted near the central place. We choose

$$F(x) = \frac{1}{1 + \exp(-15|x| + 3)} \tag{4.2.3}$$

such that $F(x) \neq 0$ for all x. Figure 4.6, Figure 4.7, and Figure 4.8 show that the shape of the distribution of consumers has either two symmetric humps on both sides or a single hump centred at $x = 0$ depending on the parameters we choose. These figures also illustrate that various values of parameters affect the way consumers disperse. At $\alpha = 10$, $\beta = 0.1$, $\gamma = 1$, the foraging kernel has one hump at the centre where the consumer forages at mean average distance 0.0496 from the centre with variance 0.002. If we decrease α to be 3, the settling rate decreases and the kernel

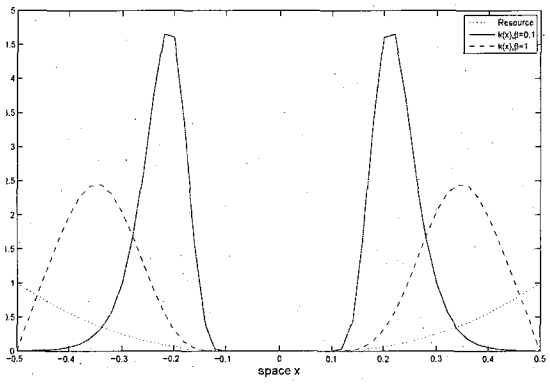

Figure 4.5: The resource-dependent foraging kernels at $\beta = 0.1$ (solid) and $\beta = 1$ (dashed) with fixed $\alpha = 10$, $\gamma = 2$ for the non-homogeneous resource distribution (4.2.2). Both kernels have two humps symmetrically placed on both sides.

has 2 humps as illustrated in Figure 4.6. In this case, the mean distance increases to 0.0856 with variance 0.0052. If we increase β to 1, the settling rate decreases and the kernel has 2 humps as shown in Figure 4.7. The mean distance increases to 0.1063 with variance 0.0055. Next, Figure 4.8 shows that if we increase γ to 10, the kernel has obvious two humps. Here, the mean distance is 0.0808 with variance 0.0012.

In conclusion, the uniform resource distribution results in the Laplace kernel. The non-homogeneous resource distribution (4.2.2) produces a 2-peaked kernel. In contrast, another non-homogeneous resource distribution (4.2.3) can produce either 2-peaked kernel or single-peaked kernel. In this case, there are still some consumers foraging at the centre. Except for very low resource, a smaller value of α, a smaller value of γ, or a larger value of β results in a lower settling rate. With a lower settling rate, consumers tend to move farther from the less abundant resource area and we thus observe 2-peaked kernels.

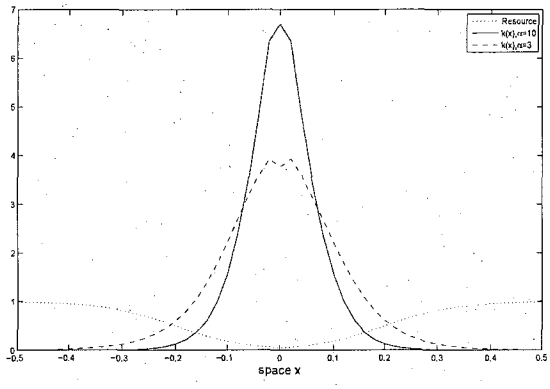

Figure 4.6: The resource-dependent foraging kernels at $\alpha = 3$ (dashed, 2 humps) and $\alpha = 10$ (solid, single hump) with fixed $\beta = 0.1$, $\gamma = 2$ for the non-homogeneous resource distribution (4.2.3).

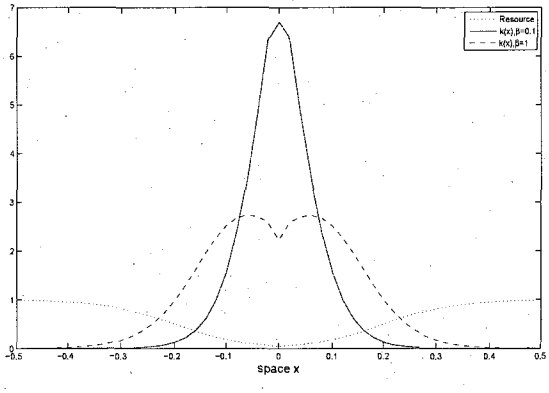

Figure 4.7: The resource-dependent foraging kernels at $\beta = 0.1$ (solid, single hump) and $\beta = 1$ ((dashed, 2 humps)) with fixed $\alpha = 10$, $\gamma = 2$ for the non-homogeneous resource distribution (4.2.3).

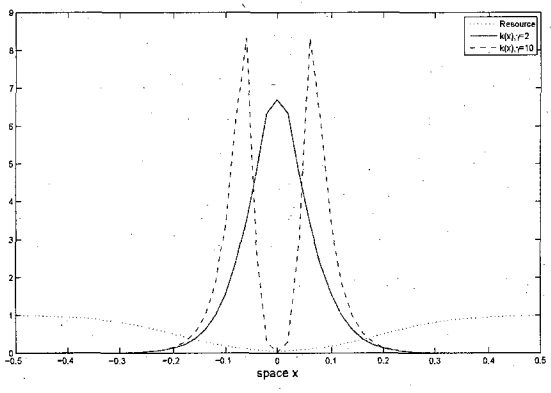

Figure 4.8: The resource-dependent foraging kernels at $\gamma = 2$ (solid, single hump) and $\gamma = 10$ (dashed, 2 humps) with fixed $\alpha = 10$, $\beta = 0.1$ for the non-homogeneous resource distribution (4.2.3).

Chapter 5

Population Dynamics with Resource-Dependent Settling Kernel

We studied the relation between the resource-dependent foraging kernel derived from a pair of PDEs (4.1.3), (4.1.4) and fixed resource distributions. In this chapter, we add the dynamics of consumer-resource interaction. The kernel $k_t(x)$ is thus not fixed in time as an individual's decision of settling is based on the availability of resource at time t. Here, we apply the Beverton-Holt growth function and the negative exponential function to our consumer-resource model. The spatial consumer-resource model with the resource-dependent kernel is given by

$$F_{t+1}(x) = \frac{rF_t(x)}{1+\frac{r-1}{K}F_t(x)}e^{-a_F C_t k_t(x)}, \tag{5.0.1}$$

$$C_{t+1} = sC_t + \tilde{b}\int_{-L/2}^{L/2}\frac{rF_t(x)}{1+\frac{r-1}{K}F_t(x)}[1-e^{-a_F C_t k_t(x)}]e^{-a_R|x|}dx, \tag{5.0.2}$$

where $k_t(x)$ is determined in each time step according to the PDEs model (4.1.3), (4.1.4) with settling rate (4.2.1). We introduce the non-dimensional quantities and

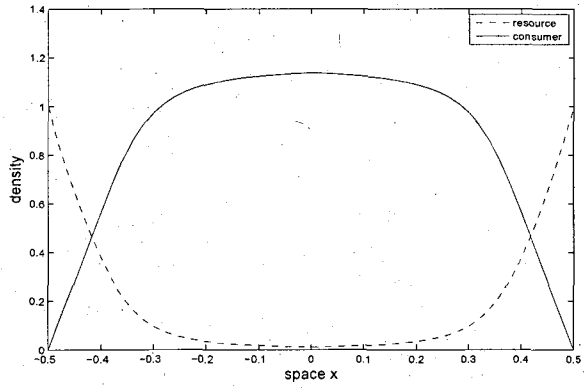

Figure 5.1: Foraging kernels at different time steps with fixed $r = 2.5$, $s = 0.5$, $b = 8$, $\beta = 0.1$, $\gamma = 1$, $a_R = 2$. At the stable steady state, the resource-dependent kernel has a single hump at the central location.

the model becomes

$$f_{t+1}(x) = \frac{r f_t(x)}{1 + (r-1) f_t(x)} e^{-c_t k_t(x)}, \tag{5.0.3}$$

$$c_{t+1} = s c_t + b \int_{-1/2}^{1/2} \frac{r f_t(x)}{1 + (r-1) f_t(x)} [1 - e^{-c_t k_t(x)}] e^{-a_R|x|} dx. \tag{5.0.4}$$

This model can exhibit a stable coexistence equilibrium or limit cycles, as numerical simulations reveal. In all simulations, we find that if the coexistence steady state is stable, then the corresponding foraging kernel has a single hump at the central location (see Figure 5.1 for an example).

In Figure 5.2 we illustrate how the foraging kernel can change over a limit cycle. We set $\alpha = 1$ and $D = 0.01$ in the two PDEs (4.1.3)(4.1.4) so that for $\beta = 0$, the kernel $k(x) = \frac{10e^{-10|x|}}{2}$ is the Laplace kernel and $\int_{-L}^{L} k(x)dx > 0.98$. We apply the distance-discounting function $R(x) = \exp(-a_R|x|)$ introduced in Chapter 1.

Figure 5.2 shows various resource-dependent foraging kernels at $t = 2000$, 2003, 2006, 2009, 2012 in the model (5.0.3), (5.0.4). Consumers move separatly from the central place while the resources near the central place is low. Then the consumers

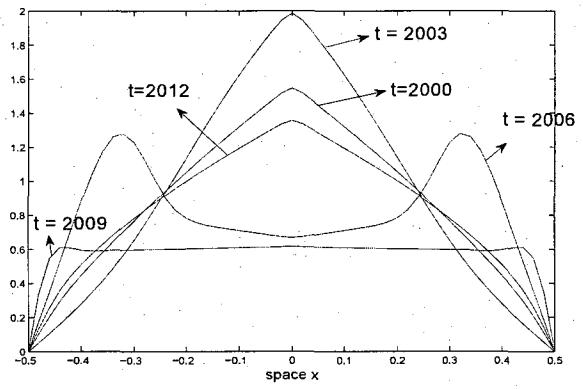

Figure 5.2: Foraging kernels at different time steps with fixed $r = 2.5$, $s = 0.5$, $b = 8$, $\beta = 0.1$, $\gamma = 1$, $a_R = 1$. These foraging kernels have either two symmetric humps or one single hump depending on the availability of resource near the central place.

return back to the central place when resources grow to a sufficient level. The resources near the central place decline as there are too many consumers, and the whole process starts over again.

5.1 Parameters from the Growth Dynamics

Similar to the model with fixed foraging kernels, the parameters related to the growth dynamics affect the stability of the coexistence equilibrium. We know that the survival rate s in the model with the Laplace kernel has the opposite effect on the stablity to the model with the uniform kernel. In contrast, the other two parameters r and b in the models with these fixed kernels have the same effect on the stability. In the model with the resoure-dependent kernel, these parameters could have the same effects as well as the opposite or mixed effects.

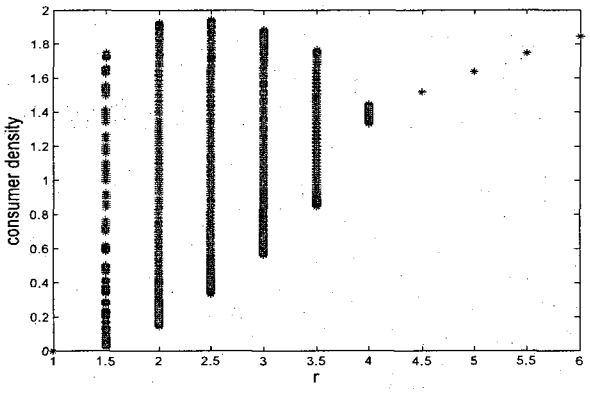

Figure 5.3: Bifurcation of model (5.0.3), (5.0.4) for increasing r with fixed $s = 0.5$, $b = 8$, $\beta = 0.1$, $\gamma = 1$, $a_R = 1$. A Neimark-Sacker bifurcation is observed as r decreases.

Net Reproductive Rate r

In the models with the fixed uniform or the Laplace kernels, the coexistence equilibrium is stable if the value of r is sufficiently high (provided we have compensatory growth of the resource). From numerical simulations, we find that the influence of r on the stability is consistent: a higher value of r in the model (5.0.3)(5.0.4) also leads the solution to converge to a stable coexistence equilibrium. Figure 5.3 shows that the consumer density oscillates with a bounded amplitude for smaller values of r. This amplitude decreases as r increases and the consumer density eventually converges to a stable steady state.

Conversion Coefficient b

Too many consumer offspring produced each year result in the lack of available resources for consumers in the following year. In the model (5.0.3), (5.0.4), we thought resource and consumer populations could reach a stable steady state with a large value of b for most sets of other parameters as consumers can find a foraging location

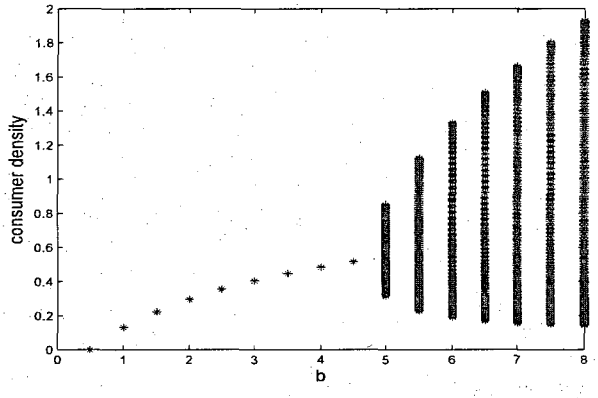

Figure 5.4: Bifurcation of model (5.0.3), (5.0.4) for increasing b with fixed $s = 0.5$, $r = 2$, $\beta = 0.1$, $\gamma = 1$, $a_R = 1$. A Neimark-Sacker bifurcation is observed as b increases.

where there are sufficent resources. However, we find that the parameter b in the model (5.0.3), (5.0.4) has the same effect on the stabiltity of the coexistence equilibrium as it has in the models with fixed kernels: a smaller value of b stablizes the equilibrium. Figure 5.4 illustrates that the consumer density converges to a stable steady state after a long time for smaller values of b. If we increase b, the population will oscillate in a limit cycle. The amplitude of oscillation increases as b increases.

Survival Rate s

Smaller values of s in the model with the uniform kernel stablizes the coexistence equlibrium. In contrast, smaller values of s in the model with the Laplace kernel lead the consumer density to limit cycles. According to some of our numerical simulations, we find that s in the model (5.0.3)(5.0.4) has the same effect as s in the model with the Laplace kernel: smaller values of s result in limit cycles and the solution converges to a stable steady state when the value of s is large enough as shown in Figure 5.5.

We have known that smaller values of b stablize the system. In other simulations,

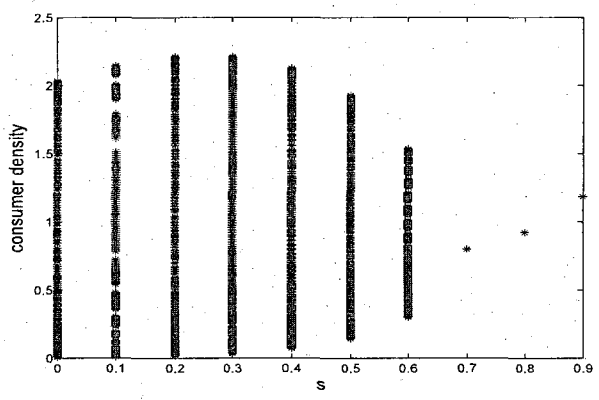

Figure 5.5: Bifurcation of model (5.0.3), (5.0.4) for increasing s with fixed $r = 2$, $b = 8$, $\beta = 0.1$, $\gamma = 1$, $a_R = 1$. A Neimark-Sacker bifurcation is observed as s decreases.

we reduce b to 5 for example, but keep other values of parameters the same and expect that the solution would converges to a stable steady state for smaller values of s. Figure 5.6 shows that the equilibrium becomes stable for s being less than 0.3. However, we still observe limit cycles for s is between 0.4 and 0.6.

5.2 Parameters from the Foraging Kernel

Parameters associated with the settling rate decide the shape of resource-dependent foraging kernel. Consumers with low settling rate tend to move farther to forage and therefore form a two-peaked kernel. On the other hand, consumers settle at the place with low resource if the value of β is small, i.e. the settling rate is large. From Figure 5.7, we observe that the consumer density oscillates in this case (smaller values of β). If we increase β so that the settling rate is not so high, the consumer moves farther to find a more resource-rich place to forage and the population converges to a stable steady state.

When the resource is low (see Figure 4.1), a higher value of γ gives a lower settling

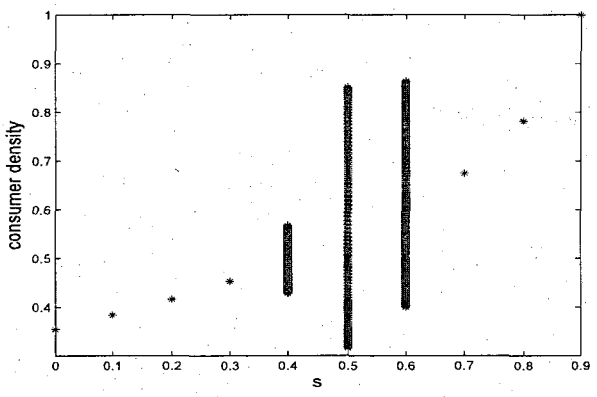

Figure 5.6: Bifurcation of model (5.0.3), (5.0.4) for increasing s with fixed $r = 2$, $b = 5$, $\beta = 0.1$, $\gamma = 1$, $a_R = 1$. Limit cycles are observed for r being in the range 0.4 and 0.6.

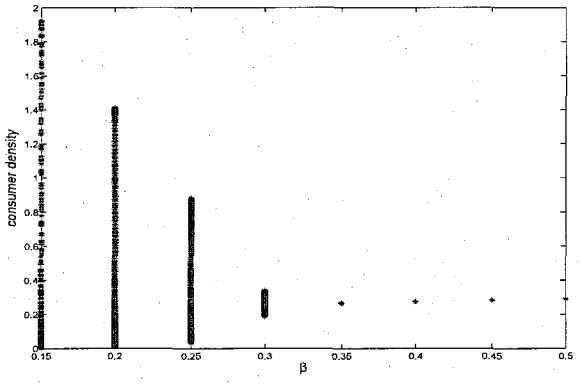

Figure 5.7: Bifurcation of model (5.0.3), (5.0.4) for increasing β with fixed $s = 0.5$, $b = 15$, $r = 1.2$, $\gamma = 1$, $a_R = 1$. A Neimark-Sacker bifurcation is observed as β decreases.

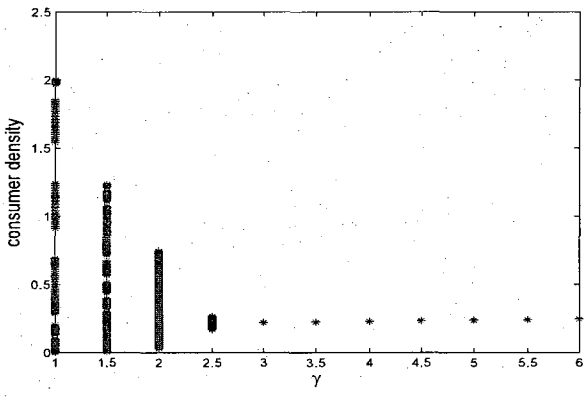

Figure 5.8: Bifurcation of model (5.0.3), (5.0.4) for increasing γ with fixed $s = 0.5$, $b = 11$, $r = 1.2$, $\beta = 0.1$, $a_R = 1$. A Neimark-Sacker bifurcation is observed as γ decreases.

rate. Therefore, we expect the value of γ and the value of β should have the same effect on the stability. As shown in Figure 5.8, the consumer population converges to a stable steady state for a larger value of γ but it oscillates with a bounded amplitude for a smaller value of γ. The amplitude increases as γ decreases.

5.3 The Parameter Related to Distance Discount

The growth in consumer population is proportional to the amount of resources they foraged in the previous year. However, the farther the foraging location is from the central place, the more energy is required to reach the resource. This causes a reduction of the consumer's breeding success. Figure 5.9 shows that the consumer density converges to a stable steady state from a limit cycle as a_R increases. Hence, if the distance that consumers travel has a more significant impact, i.e. the value of a_R is larger, the consumer density tends to have a stable steady state. We also expect that the consumer density decays as the value of a_R increases according to equation (5.0.4) and Figure 5.9.

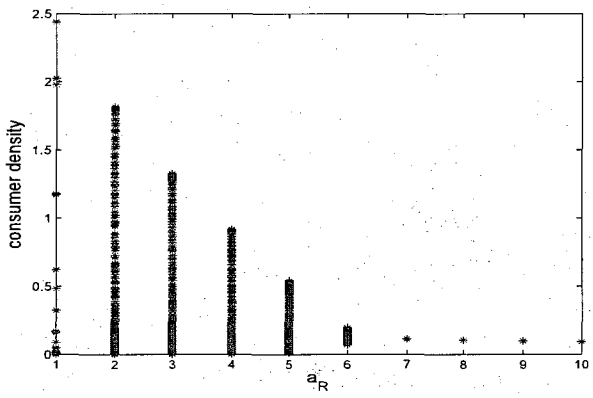

Figure 5.9: Bifurcation of model (5.0.3), (5.0.4) for increasing a_R with fixed $s = 0.5$, $b = 15$, $r = 1.2$, $\beta = 0.1$, $\gamma = 1$. A Neimark-Sacker bifurcation is observed as a_R decreases.

5.4 Summary

A lower resource growth rate is not able to provide sufficient food to consumers. Higher conversion coefficient results in more breedings of consumers and it might cause the situation that there is not enough food for the next generation. We find that the consumer population oscillates in a limit cycle with a lower value of r or a higher value of b. The survival rate has the mixed effect on the stability. A limit cycle can be observed for smaller values of s, or only for a certain range of values of s depending on the values of other parameters

Consumers can forage at a place with low resources if the settling rate is sufficiently high. Our simulations suggest that resource and consumers population oscillate in limit cycles if the settling rate is high. In the other words, higher values of β or γ makes the consumer density to converge to a stable steady state. Finally, we find that the model (5.0.3), (5.0.4) can be stablized by considering the distance discount for consumers' reproduction. Both populations converge to stable steady states with higher values of a_R.

Chapter 6

Conclusion and Future Work

There are three parameters directly related to the population dynamics for all models: (1) the resource growth rate r; (2) the conversion coefficent relating consumed biomass to new adult consumers b; (3) the consumer survival rate s. We concentrate here on the situation where a compensatory growth function is applied and the coexistence steady state is not always stable or unstable for all parameters. The resource with a slower growth rate may not be able to provide sufficient food for consumers on time. The system with a small value of r thus may have limit cycles for resource and consumer populations. Similarly, consumers with a higher conversion coefficient may breed too fast but resources around the habitat cannot afford their consumption. Hence, a high value of b causes resource and consumer populations to oscillate in limit cycles. The effects of consumer survival rate are different in different models. For the models where consumers disperse uniformly on the resource patch, a higher survival rate means more consumption of resources in the next generation. The situation that there is not enough food happens, so resource and consumer populations fall into limit cycles with a high value of s. In contrast, for the model with the fixed Laplace kernel, consumers near the central place do not obtain any food as the resource near the central place is completely depleted. Hence, consumers need a higher survival

rate to maintain their population level. Resource and consumer populations converge to stable steady state for a high value of s. For the model where consumers' decision on where to forage is based on the abundance of resource, the foraging kernel can have a single hump at the central place or two humps at the equal distance from the centre. The survival rate can have various effects on the stability depending on other parameters. Limit cycles of resource and consumer populations can occur for a value of s being small or in a certain range.

Consumer aggregation provides a partial refuge for the resource in low density patch (Chapter 4 in [13]). The clumped search by consumers stablizes the system for fixed kernels. The foraging kernel influenced by the consumer settling rate has a similar effect on stability. Consumers who tend to forage at the place with more abundant resources can have a stable steady state population. Equivalently, parameters that reduce the settling rate (a high value of β, for instance) lead resource and consumer populations to converge to stable steady states. In addition, the consideration of travelling distance also affects stability. For the model with a high value of energy-reduction coefficient a_R, the the number of offspring declines significantly as the distance between the foraging location and the centre increases. However, a large value of a_R results in stable equilibria for resource and consumer populations.

We have seen that fixed foraging kernels fail to reflect the impact of resource depletion. Consumers should at least forage at the place where resources exist. In addition, consumers spend energy to travel to foraging locations. The longer their search lasts, the more willing they might be to settle for non-optimal resources. Also, the rate of settling might also be determined by how many individuals are already foraging in a given area.

We could include the above two considerations into our PDE framework to determine the foraging kernel. One such possibility would be to write the settling rate as

$$a(v, F, t) = \eta \tanh\left(\frac{F}{v}\right) e^{\xi t}, \tag{6.0.1}$$

where v is the number of settled individuals; η and ξ are some constants. We could also consider individual's biased movement which towards higher resource density for a more realistic consumer-resource model. These scenarios are left for future research.

Bibliography

[1] L. J. S. Allen, An Introduction to Mathematical Biology, Pearson Education, Inc. Upper Saddle River, NJ, (2007).

[2] C. J. Briggs, M. F. Hoopes, Stabilizing Effects in Spatial Parasitoid-Host And Predator-Prey Models: A Review, *Theoretical Population Biology*, **65** (2004), pp. 299-315.

[3] P. D. Boersma, G. A. Rebstock, E. Frere, S. E. Moore, Following the Fish: Penguins and Productivity in the South Atlantic, *Ecological Monographs*, **79** (2009), pp. 59-76.

[4] E. L. Charnov, Optimal Foraging, the Marginal Value Theorem, *Theoretical Population Biology*, **9** (1976), pp. 129-136.

[5] B. Culik, Finding Food in the Open Ocean: Foraging Strategies in Humboldt Penguins, *Zoology*, **104** (2001), pp. 327-328.

[6] L. A. Dugatkin, Principles of Animal Behavior, W. W. Norton Company, Inc. New York, NY, (2004).

[7] L. Edelstein-Keshet, Mathematical Models in Biology, SIAM, Philadelphia, PA, (2005).

[8] R. L. Fournier, Basic Transport Phenomena in Biomedical Engineering, Taylor and Francis, Philadelphia, PA, (1999).

[9] W. F. Fagan, F. Lutscher, K. Schneider, Population and Community Consequences of Spatial Subsidies Derived from Central-Place Foraging, *American Naturalist*, **170** (2007), pp. 902-915.

[10] S. A. H. Geritz, E. Kisdi, On the mechanistic underpinning of discrete-time population models with complex dynamics, *Journal of Theoretical Biology*, **228** (2004), pp. 261-269.

[11] J. Guckenheimer, and P. Holmes, Nonlinear Oscillations, Dynamical Systems, and Bifurcations of Vector Fields, Springer-Verlag, New York, NY, (1983).

[12] C. S. Holling, Some Characteristics of Simple Types of Predation and Parasitism, *Canadian Entomologist*, **91** (1959), pp. 385-398.

[13] M. P. Hassell. The Dynamics of Arthropod Predator-Prey Systems, Princeton University Press, Princeton, New Jersey, (1978).

[14] K. Johst, R. Brandl, R. Pfeifer, Foraging in a Patchy and Dynamic Landscape: Human Land Use and the White Stork, *Ecological Applications*, **11** (2001), pp. 60-69.

[15] P. M. Kareiva, Local Movement in Herbivorous Insects: Applying a Passive Diffusion Model to Mark Recapture Field Experiments, *Oecologia*, **57** (1983), pp. 322-327.

[16] M. Kot, Elements of Mathematical Ecology, Cambridge University Press, Cambridge, UK, (2001).

[17] A. J. Lotka, Undamped Oscillations Derived from the Law of Mass Action, *Journal of the American Chemical Society*, **42** (1920), pp. 1595-1599.

[18] A. J. Lotka, Elements of Physical Biology, Williams and Wilkins, Baltimore, MD, (1925).

[19] R. M. May, Simple Mathematical Models with Very Complicated Dynamics, *Nature*, **261** (1976), pp. 459-467.

[20] R. M. May, Host-Parasitoid Systems in Patchy Environments: A Phenomenological Model, *Journal of American Ecology*, **47(3)** (1978), pp. 833-844.

[21] J. D. Murray. Mathematical Biology I: An Introduction, Interdisciplinary applied mathematics, Springer, New York, NY, (2002).

[22] W. W. Murdoch, C. J. Briggs, and R. M. Nisbet, Consumer-Resource Dynamics, Princeton University Press, Princeton, NJ, (2003).

[23] A. J. Nicholson, V. A. Bailey, The Balance of Animal Populations, Part I, *Proceedings of Zoological Society of London*, **3** (1935), pp. 551-598.

[24] M. G. Neubert, M. Kot, The Subcritical Collapse of Predator Populations in Discrete-Time Predator-Prey Models, *Mathematical Biosciences*, **110** (1992), pp. 45-66.

[25] M. G. Neubert, M. Kot, M. A. Lewis, Dispersal and Pattern Formation in a Discete-Time Predator-Prey Model, *Theoretical Population Biology*, **48** (1995), pp. 7-43.

[26] G. H. Orians, N. E. Pearson, On the Theory of Central-Place foraging, pp. 154-177 in D. J. Horn, R. D. Mitchell, G. R. Stairs, eds, Analysis of Ecological Systems, Ohio State University Press, Columbus, OH, (1979).

[27] G. A. Parker, R. A. Stuart, Animal Behavior as a Strategy Optimizer: Evolution of Resource Assessment Strategies and Optimal Emigration Thresholds, *American Naturalist*, **110** (1976), pp. 1055-1076.

[28] W. E. Ricker, Stock and Recruitment, *Journal of the Fisheries Research Board of Canada*, **11** (1954), pp. 559-623.

[29] T. R. Raffel, N. Smith, C. Cortright, A. J. Gatz, Central Place Foraging by Beavers (Castor Canadensis) in a Complex Lake Habitat, *The American Midland Naturalist*, **162** (2009), pp. 62-73.

[30] J. P. Smith, Foraging Flights and Habitat Use of Nesting Wading Birds (Ciconiiformes) at Lake Okeechobee, Florida, *Colonial Waterbirds*, **18** (1995), pp. 139-158.

[31] S. H. Strogatz, Nonlinear Dynamcis and Chaos Westview Press, Cambridge, MA, (1994).

[32] P. F. Verhulst, Notice sur la loi que la Population suit dans son accroissement, *Correspondance mathmatique et physique*, **10** (1838), pp. 113-121.

[33] V. Volterra, Fluctuation in the Abundance of a Species Considered Mathematically, *Nature*, **118** (1926), pp. 558-560.

[34] G. de Vries, T. Hillen, M. Lewis, J. Muller, and B. Schonfisch, A Course in Mathematical Biology: Quantitative Modeling with Mathematical and Computational Methods, Mathematical Modeling and Computation, SIAM, Philadelphia, PA, (2006).

[35] S. Wiggins, Introduction to Applied Nonlinear Dynamical Systems and Chaos, Springer-Verlag, New York, NY, (2003).

Appendix: Matlab Code for the Consumer-Resource Model

```
clear all;

% coefficients of consumer-resource model
s = 0.5;
b = 8;
yearmax = 2000;
L = 0.5;

% coefficents of resource growth
r = 2.5;
K = 1;

% coefficients of searching efficiency and distance discount
af = 1;
ar = 1;

% parameters used in the finite difference method
Nx = 50;
```

```
dx = 2*L/Nx;
T = 400;
D = 0.01;
dt = dx^2/(5*D);
mu = D*dt/(dx)^2;

% coefficients of resource-dependent kernal
alpha = 1;
gamma = 1;
beta = 0.1;

% initial
F = ones(Nx+1, 1);
I = zeros(Nx+1, 1);
a = zeros(Nx+1, 1);
C = 0.1;

% distance discount
xj = -L:dx:L;
R = exp(-ar*abs(xj));
R = R';

for year = 1:yearmax

% I.C. for the finite difference method
u = zeros(Nx+1, 1);
utemp = zeros(Nx+1, 1);
v = zeros(Nx+1, 1);
```

```
u(Nx/2+1, 1) = 1/dx;

a = alpha*F.ĝamma./(betaĝamma+F.ĝamma); % resource-dependent settling rate

for tau = 0:dt:T
utemp = u;
for i = 2:Nx
u(i) = mu*(utemp(i+1)-2*utemp(i)+utemp(i-1)) + (1-a(i)*dt)*utemp(i); % moving
individuals
v(i) = v(i) + a(i)*u(i)*dt; % settled individuals
end
end

I = K*r*F ./ (K+(r-1)*F) .* (1-exp(-af*C*v)) .* R;
F = K*r*F ./ (K+(r-1)*F) .* exp(-af*C*v);
C = s*C + b*sum(I)*dx;

end

% plot distributions of resource and consumer
x = -L:dx:L;
plot(x, F,'g')
hold on
plot(x, v)

hold off

xlabel('x'); ylabel('densities')
```

title('Random movement, resource-dependent settling')